Ending the Covid-19 pandemic[*]

Phurichai Rungcharoenkitkul[†]

Bank for International Settlements

February 28, 2021

For latest version of the paper and code for updating results please go to:
https://github.com/phurichai/covid19macro

Abstract

This paper assesses the macroeconomic impact of managing the late stage of the Covid-19 pandemic, by analysing quantitatively the interactions between epidemiological and economic developments. The framework features an SEIR-type model that describes the pandemic evolution conditional on society's mobility choice, and a policy unit that chooses mobility optimally to balance lives and livelihood objectives. The model can be fit to daily data via a fast and robust empirical procedure, allowing a timely policy analysis as situation evolves. As of late February, the projected median output loss in 2021 among 27 advanced and emerging market economies is about 2% of pre-pandemic trends. This relatively benign outcome hinges on a sustained progress in vaccination and no major epidemiological setbacks. Hiccups in vaccination or a '3rd-wave' surge in infection rate could raise output loss to 4%. In the most severe scenario, virus mutations that compromise existing immunity could require more protracted lockdowns. In this case, median output loss may reach 6% in 2021 alone, with further repercussions in subsequent years.

JEL Classification: E00, I18
Keywords: Covid-19 pandemic, health-economic tradeoffs, SEIR model, lockdown, vaccines

1 Introduction

The Covid-19 pandemic is both a global health and economic crisis. At the time of writing, more than 2.5 million lives have been lost to the disease, nearly 1 million of which happened over the last few months alone as a result of the second infection wave. In a bid to save lives, authorities around the world have had to put up drastic measures to restrict human interactions and curb the virus spread, extending them as needed to suppress resurgence of cases. These measures, while necessary from the public health standpoint and may be the only means to put an end to the crisis, have led to macroeconomic consequences of truly historic proportions. Output losses during the 'great lockdown' of 2020 are as high as 8% on average, exceeding even the sharp contraction associated with past financial crises. The macroeconomic damages are higher still for those reliant on most affected sectors, such as tourism and services.

The arrival of vaccines in late 2020 ushered in a new phase of the pandemic and opened up the possibility of a quick and smooth 'pandexit'. After showing high efficacy in trials, several vaccines are being quickly rolled out in a number of countries, particularly in advanced economies which have secured most of available dosages. At the same time, there remain significant challenges and risks in the months ahead. If the production and take-up of vaccines disappoint, economic activity could suffer again. Virus mutations could also present unpredictable new challenges, possibly negating the effects of vaccines. Should these downside risk scenarios play out, what could be the resulting macroeconomic consequences? How much and how long should lockdowns and mobility restrictions be expected? These questions are clearly of first-order importance for macroeconomists and those in charge of fiscal, monetary and regulatory policies.

This paper provides a analytical and data-driven framework to assess macroeconomic impact during the last lap of the pandemic. The framework consists of two interdependent blocs, designed to capture the interactions between the pandemic evolution and economic decisions. The first is an SEIR model describing the epidemiological dynamics, featuring time-varying infection and death rates which depend on public policy and societies' behaviour. The second bloc describes how societies react to pandemic developments, by choosing the level of mobility to strike a balance between limiting deaths and containing economic disruptions. Together, the two blocs provide a structural description of how the pandemic and economic activity co-evolve. The resulting dynamic system can then be used to formulate projections, conduct policy analysis and examine implications of various pandemic scenarios.

Understanding how the pandemic evolution and economic decisions interact is central to key policy issues at present. How quickly could countries lift their lockdown measures depend precisely on these considerations. How much vaccination is needed to attain 'herd immunity' depends not only on how many susceptible people remain in the population, but also how actively they interact with potentially infectious individuals. The latter is a function of economic activity, in turn a reflection of how the society reacts to the pandemic. The approach in this paper makes this interdependence explicit, which is essential given the pervasive relevance of economic considerations in designing policies to tackle the pandemic.

An important focus of the paper is to provide a flexible and robust empirical routine for fitting the model to data, allowing a fast simultaneous update across a wide range of countries as daily information becomes available. This is achieved via a 2-step algorithm. In the first

step, the SEIR model and the data are used to filter out the time-varying infection and death rates in a non-parametric way, which involves negligible computational costs. The second stage involves a parametric modelling of these filtered series, which provides the basis for constructing out-of-sample forecasts. For the infection rate, this step entails estimating the contribution from mobility to the infection rate. The determination of mobility is then the domain of the second policy bloc, which is characterised analytically to save computational times. Implementing a complete update and producing forecasts for 27 advanced and emerging market economies takes only a few minutes.

The fitted model can produce forecasts under various epidemiological scenarios. Three are considered: a resurgence of infection rate unrelated to mobility ('3rd wave'), a stall in vaccination, and virus mutations that cause reinfection. The macroeconomic implications of these scenarios in terms of annual GDP losses are notable, particularly in the case of reinfection. At the same time, the degree of vulnerability to these scenarios differs across countries. Those making slower progress in vaccination are particularly exposed to any resurgence of infection rate for example.

The paper is organised as follows. Section 2 presents the model, detailing the two blocs. Section 3 describes the empirical procedure and the construction of projections. Simulation results as well as scenarios are discussed in section 4, before section 5 concludes.

2   The model

2.1   The epidemiological model

The epidemiological model is an enriched SEIR variety, building on Li et al. (2020) with several key extensions. The system features 12 differential equations and state variables:

$$\Delta S_{t+1} = -\gamma_t S_t I_t / N + r_{re}(R_t + V_t) - r_v \tag{2.1}$$

$$\Delta E_{t+1} = \gamma_t S_t I_t / N - r_i E_t \tag{2.2}$$

$$\Delta I_{t+1} = r_i E_t - r_d I_t \tag{2.3}$$

$$\Delta U D_{t+1} = r_d p_{dth,t}(1 - p_d) I_t - r_{dth} U D_t \tag{2.4}$$

$$\Delta Q D_{t+1} = r_d p_{dth,t} p_d (1 - p_h) I_t - r_{dth} Q D_t \tag{2.5}$$

$$\Delta H D_{t+1} = r_d p_{dth,t} p_d p_h I_t - r_{dth} H D_t \tag{2.6}$$

$$\Delta U R_{t+1} = r_d (1 - p_{dth,t})(1 - p_d) I_t - r_{ri} U R_t \tag{2.7}$$

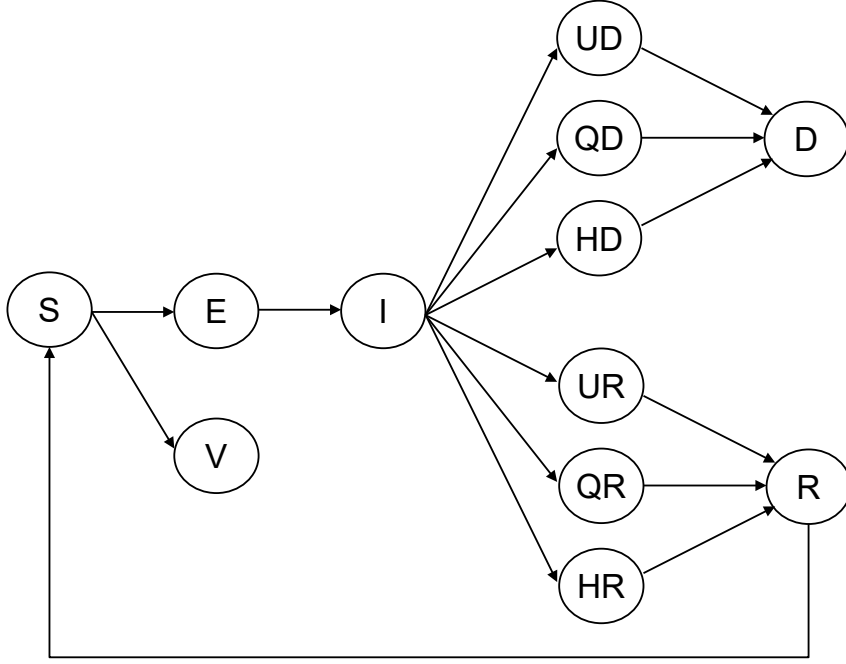$$\Delta Q R_{t+1} = r_d (1 - p_{dth,t}) p_d (1 - p_h) I_t - r_{ri} Q R_t \tag{2.8}$$

$$\Delta H R_{t+1} = r_d (1 - p_{dth,t}) p_d p_h I_t - r_{rh} H R_t \tag{2.9}$$

$$\Delta R_{t+1} = r_{ri}(U R_t + Q R_t) + r_{rh} H R_t - r_{re} R_t \tag{2.10}$$

$$\Delta D_{t+1} = r_{dth}(U D_t + Q D_t + H D_t) \tag{2.11}$$

$$\Delta V_{t+1} = r_v - r_{re} V_t \tag{2.12}$$

Table 1 documents the model notations, while Figure 1 shows the schematic of transitions between various states.

Note: Arrows denote the direction of population flow from states. See Table 1 for explanation of notations.

Figure 1: Model schematic

The mechanism of the model is similar to that of the basic SEIR models. Each period, $\gamma_t S_t I_t / N$ new infections emerge, representing the number of susceptible individuals S_t who catch the virus and transition to the exposed type E_t. These new infections arise from contacts between susceptible and infectious groups governed by the aggregate matching function $S_t I_t / N$ multiplied by the infection rate γ_t.[1] The exposed people E_t become infectious after some virus incubation period. The infectious individuals I_t can pass the virus along to susceptible ones, until they are detected at rate r_d and join one of the six quarantine states, $\{UD_t, QD_t, HD_t, UR_t, QR_t, HR_t\}$. These additional states, not present in the barebone SEIR model, are included to better fit the model to observed data. They are divided into those that self-isolate at home (UD_t, UR_t), those that are placed under quarantine after confirmed by official tests (QD_t, QR_t) and those that hospitalised after testing positive (QD_t, QR_t). People exit quarantine either by recovering (joining R_t) or dying (joining D_t), and are pre-allocated by at the quarantine stage.

As in the simple SEIR model, the dynamics of infections depend primarily on two factors: how infectious the disease is, and how many people are susceptible to it. Specifically, the virus spreads faster than it dies out if the pool of infected individuals $(E_t + I_t)$ is growing, namely if

$$\frac{\gamma_t}{r_d}\frac{S_t}{N} > 1 \tag{2.13}$$

At the start of the pandemic where $S_0/N \approx 1$, the condition becomes $\gamma_0/r_d > 1$, which motivates the definition of the basic reproductive number $R0 \equiv \gamma_0/r_d$. The left hand side of condition 2.13

---

[1] An aggregate matching function assumes random pairwise matching between individuals, satisfied when e.g. the spatial distribution of individual types is 'well-mixed'.

Table 1: SEIR model notation

States (in total number)		**Transition rates/probabilities**	
S_t	Susceptible population	γ_t	Time-varying component of infection rate
E_t	Exposed, not yet infectious	r_i	Incubation-to-infection transition rate
I_t	Infectious population	r_d	Infection-to-quarantine transition rate
UD_t	Undetected, sick at home; will die	r_{dth}	Death rate
QD_t	Detected, quarantined; will die	r_{ri}	Recovery rate
HD_t	Detected, hospitalised; will die	r_{rh}	Recovery rate, once hospitalised
UR_t	Undetected, sick at home; to recover	p_d	Probability of being detected by tests
QR_t	Detected, quarantined; to recover	p_h	Probability of being hospitalised
HR_t	Detected, hospitalised; to recover	$p_{dth,t}$	Probability of dying, once infected
R_t	Recovered population	r_v	Vaccination per unit time
D_t	Dead population	r_{re}	Reinfection rate (immunity loss)
V_t	Effectively vaccinated population		
N	Total population		

can be thought of as the effective reproductive number for arbitrary period t, which depends on the infection rate γ_t and the size of susceptible population S_t/N. There are two (non-exclusive) strategies for slowing infections - one could suppress γ_t through social distancing and lockdowns, or seek to lower the number of susceptible individuals. The latter 'herd immunity' could be achieved by simply allowing the pandemic to run its course or mass-scale vaccinations.

The infection rate γ_t is posited to consist of two parts, reflecting the influence from societies' behaviour and epidemiological properties of the virus:

$$\gamma_t = \gamma_t^m + \gamma_t^d \tag{2.14}$$

The first term γ_t^m represents the contribution from economic activity, as a more vibrant economy entails greater human interactions and a higher infection rate. It is posited to be increasing in mobility $m_t \in [-1, 0]$ (measured as a percentage deviation from the pre-pandemic level):

$$\gamma_t^m = \beta_0 \exp(\beta_1 m_t) \tag{2.15}$$

The functional form recognises potential nonlinearity, as the rate of infections may decline less than one for one with overall mobility (e.g. due to superspreaders). This term captures the central tradeoff between lives and livelihood facing the policymaker - slowing down infections requires lower mobility and economic activity.

The auxiliary term γ_t^d captures all other time-varying determinants of the infection rate unrelated to mobility. It picks up the effects of health precautions such as mask wearing, hand washing and social distancing in daily lives which can reduce the infection rate without disrupting economic activity. It also includes infection rate 'shocks' owing to seasonal patterns of the virus, greater human contact during festive seasons (conditional on mobility), importations of cases from other countries, and virus mutations. For baseline out-of-sample policy simulation, γ_t^d is posited to follow a mean-reverting process:

$$\gamma_t^d = \rho \gamma_t^d + \epsilon_t \tag{2.16}$$

where ϵ_t is white noise, and ρ can be estimated using the past data. One could also construct scenarios of a new virus strain associated with a higher infection rate, by assuming a persistent shock to ϵ_t.

The model features an *effectively vaccinated* group, V_t, namely the people who successfully obtain immunity from vaccines rather than through being exposed to the virus. The first effect of vaccination is to directly subtract from the susceptible group, a shortcut to immunity as depicted in Figure 1, and accelerate the achievement of herd immunity without incurring deaths. The second effect of inoculation depends on how the vaccine is distributed. Prioritising the distribution to the elderly population with the highest fatality rate would reduce the overall fatality rate. This effect could be explicitly quantified using the demographic data, as done below. There are also other possible strategies of distributing the vaccines. For instance, vaccinating the group which are more likely to interact with others, such as healthcare professionals, frontline workers or younger population could contribute to lowering the infection rate. Introducing these effects into the model could be done in principles by linking vaccinations to γ_t, but is not attempted below. Vaccinations received after exposure are assumed to be ineffective, hence there is no transition path from state E_t to V_t (such transition can be easily introduced however if an interim vaccination later proves effective). Both recovered and vaccinated population are assumed not to be silent carriers.[2]

The death probability conditional on infection is posited to be:

$$p_{dth,t} = (1 + \eta(\xi_t - 1))\tilde{p}_{dth,t} \tag{2.17}$$

$\tilde{p}_{dth,t}$ is the underlying death probability which varies with epidemiological factors and sanitary standards, but does not take into account the effect of targeted vaccination allocation. It includes the effects of improved health professionals' proficiency in dealing with the Covid-19 patients, which may have led to falling fatality rates since the start of the pandemic in many countries. It also captures the effects of virus mutations and ICU occupancy rate which may push up $p_{dth,t}$. Next, $\xi_t \in [0,1]$ is the death-reduction factor under a perfectly targeted distribution strategy with vaccines allotted to population in descending order of their ages. ξ_t is a function of Covid-19's age-specific fatality probability $p_{dth}^*(age)$, the age distribution F and the size of vaccinated population V_t/N:

$$\xi_t = \int_0^{F^{-1}(1-V_t/N)} p_{dth}^*(age)dF(age) \tag{2.18}$$

The parameter $\eta \in [0,1]$ controls the degree to which countries' actual vaccine distribution conforms to this ideal targeted strategy.[3] With $\eta = 1$, the death probability is equal to the theoretical lower bound $\xi_t\tilde{p}_{dth,t}$, while $\eta = 0$ implies random vaccine distribution and $p_{dth,t} =$

---

[2] Immune people could harbour the virus (e.g. in their nasal cavities) and able to transmit it to others. Accounting for this mode of transmission within the model is possible, and entails splitting R_t and V_t into carrier and non-carrier sub-types. As it remains uncertain how prevalent this silent transmission is, I do not attempt the exercise here.

[3] In some countries, the elderly have in fact been purposely excluded, given concerns about the vaccine effectiveness for their group. As mentioned, other vaccination strategies, e.g. involving front-line workers, have also been adopted.

$\tilde{p}_{dth,t}$.

The model allows for the possibility that the recovered population may eventually lose their immunity and become susceptible again. While so far rare, reinfections have been confirmed in several cases and it is possible for people to lose their immunity over sufficiently long period of time. Virus mutations could also increase this likelihood by evading the immune system's detection. In the reinfection scenario considered below, I assume both the recovered and vaccinated groups could potentially lose immunity.

2.2 Mobility policy function

The society has a preference for maintaining mobility (a proxy for economic activity) and avoiding additional deaths. At time t it chooses m_t to maximise:

$$U_{t_0} = \sum_{t=t_0}^{\infty} \left[-\left(\Delta\tilde{d}_t\right)^2 - \phi m_t^2 \right] \tag{2.19}$$

where $\phi > 0$ is the relative weight on economic activity in comparison to lives saved. I assume no discount factor and define $\Delta\tilde{d}_t$ as the additional deaths (in percent of population) attributed to mobility decisions m_t made at time t, incurred at any point in the future. The link between m_t and $\Delta\tilde{d}_t$ is dictated by the epidemiological equations 2.1-2.12. In assuming no discount factor and hence making no differentiation regarding the timing of deaths, the formulation greatly reduces the dimensionality of the problem and implies a relatively simple optimality condition as I now show.[4]

$\Delta\tilde{d}_t$ can be derived via backward induction. At any arbitrary period τ, the policymaker can tally up the number of individuals who either just pass away or will eventually do so:

$$\Delta(D_\tau + UD_\tau + QD_\tau + HD_\tau) = r_d p_{dth,t} I_{\tau-1} \tag{2.20}$$

namely it is proportional to the size of infectious population in the period prior. Summing up over all τ at which deaths could be traced back to m_t, the left-hand term becomes $\Delta\tilde{d}_t$ by definition:

$$\Delta\tilde{d}_t = r_d p_{dth,t} \sum_{\forall\tau|m_t\to\tau} I_{\tau-1} \tag{2.21}$$

while the corresponding right-hand term $\sum_{\forall\tau|m_t\to\tau} I_{\tau-1}$ is the size of infectious population that could be linked to mobility choice made at time t. Working backward to time t, the policymaker knows that its mobility choice m_t affects the flows of people into the infectious or exposed (set to be infectious in the future) pool according to:

$$\Delta(I_t + E_t) = \gamma_t S_t I_t / N - r_d I_t \tag{2.22}$$

---

[4]The optimal policy problem can also be cast in terms of balancing between current mobility and death flows at some fixed date, either current or future. The conventional dynamic programming technique could then be used in principles, as long as one assumes a discount factor strictly less than 1. But the high number of state variables means prohibitive computational costs in practice.

Equating $I_t + E_t$ implied by equation 2.22 to $\sum_{\forall \tau | m_t \to \tau} I_{\tau-1}$, one then establishes a link between m_t and $\Delta \tilde{d}_t$, which is given by

$$\Delta \tilde{d}_t = p_{dth,t} r_d i_t (1 + \gamma_t s_t - r_d) \tag{2.23}$$

where $i_t \equiv I_t / N$, $s_t \equiv S_t / N$.

The optimal policy problem is given by the maximisation of term 2.19 subject to the constraint 2.23. The first-order condition is given by

$$-\phi m_t = \Delta \tilde{d}_t \frac{\partial \Delta \tilde{d}_t}{\partial m_t} \tag{2.24}$$

The right-hand side depends on m_t via $\gamma_t = \gamma_t^m + \gamma_t^d = \beta_0 \exp(\beta_1 m_t) + \gamma_t^d$. This is particularly convenient as one only needs to keep track of s_t and i_t rather than all 12 state variables, as if the model was a stripped-down SIR type. The optimal policy can then be solved numerically as a function of s_t, i_t, $p_{dth,t}$ and γ_t^d.

3 Empirical procedure

3.1 Data and calibration

Confirmed cases and deaths

Confirmed cases and deaths are the primary observable inputs for fitting the epidemiological model to data. In the model, these correspond to DT_t and DD_t respectively, which are generally subsets of total cases $\sum_{\forall t} I_t$ and total deaths D_t. The evolution of DT_t and DD_t follow:

$$\Delta DT_t = r_d p_d I_t \tag{3.1}$$

$$\Delta DD_t = r_{dth}(HD_t + QD_t) \tag{3.2}$$

Mobility

The proxy for m_t is the average of three Google Mobility sub-indices: (i) retail and recreation, (ii) transit and (iii) workplaces. When aggregated over time, the mobility index has a strong association with the level of output. Indeed, differences in average mobility during 2020 alone explain much of cross-country variations in output losses during the period, almost 50% in R-square terms (Figure 2; also see Rungcharoenkitkul (2021)).

Mobility is translated into output losses in GDP terms using country-specific conversion factors, assuming a linear relationship between the two. The factors are ratios of cumulative forecast revisions of 2020 growth made over the course of the year (the difference between consensus GDP growth forecasts for 2020 made at the end of 2020 and those made at the start of the year) and average mobility during 2020. In graphical terms, a country's conversion factor is the slope of the line going through the origin and the country's annotation in Figure 2. This measure captures in a simple way countries' potentially different output sensitivities to mobility, for instance due to the relative importance of the services sector or reliance on external demand and international travel.
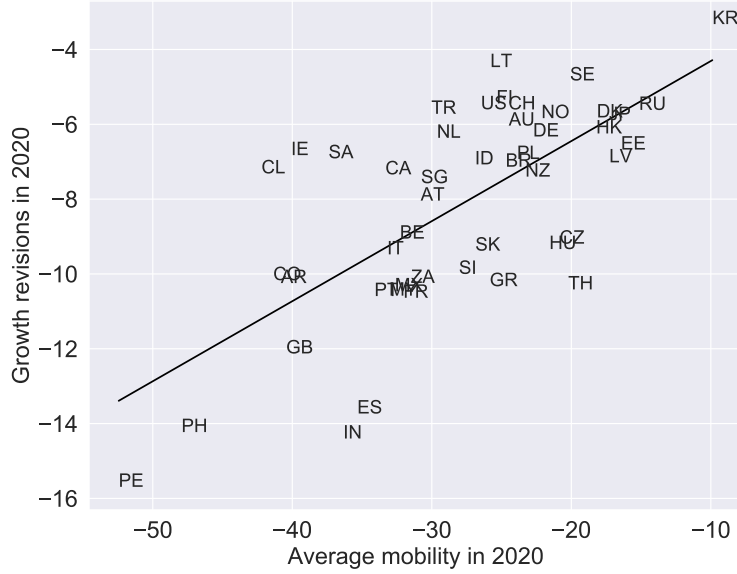
Note: 'Growth revisions in 2020' are the differences between consensus forecasts of 2020 GDP growth made at the end of 2020 and those made at the beginning of the year before Covid-19 outbreak. These could be interpreted as the total output losses from the Covid-19. The horizontal axis is the average of mobility during 2020.

Figure 2: Mobility-output relationship

Vaccination

The number of *effectively* vaccinated individuals V_t is a weighted average of partially- and fully-vaccinated groups, reflecting different degrees of immunity. For a required dosage of two injections, I assume one injection confers a 50 percent chance of immunity, while two doses are 95 percent effective at granting an immunity.[5] No attempt is made to differentiate between vaccine types. New daily effective vaccinations map to r_v in the model equation 2.12. To estimate the impact of targeted vaccine distribution on average death probability, I use age-specific fatality rates from O'Driscoll et al. (2020) and country-specific demographic data from the United Nations.

Initialising states

Initial states are guided by data and informed priors. For each country, the analysis starts when confirmed domestic cases reached or exceeded 100. Total confirmed cases and deaths on this date initialise DT_0 and DD_0 respectively, with $D_0 = DD_0/p_d$ to reflect undetected deaths and $R_0 = 5D_0$ by assumption. These imply total people under quarantine of $C_0 \equiv DT_0 - p_d(D_0 + R_0)$, which are apportioned across six quarantine states according to relative likelihood p_h and (unknown) $p_{dth,0}$. The initial death probability $p_{dth,0}$ is solved by inverting the observation equation 3.2 and substituting for HD_0 and QD_0 to match next-period death data. The initial exposed and infectious population are posited to a multiple of quarantined population: $E_0 = I_0 = kC_0/p_d$, where the unknown k is determined below. V_0 is zero as

---

[5]This assumption is motivated by the trial results of the Pfizer-BioNTech vaccine. See Polack et al. (2020).

Table 2: Initial values and calibrated parameters

Initial values			Calibrated/derived parameters		
DT_0	$=$	Confirmed cases	r_i	$=$	$\log(2)/5$
DD_0	$=$	Confirmed deaths	r_d	$=$	$\log(2)/2$
D_0	$=$	DD_0/p_d	r_{dth}	$=$	0.5
R_0	$=$	$5D_0$	r_{ri}	$=$	$\log(2)/10$
C_0	$\equiv$	$DT_0 - p_d(D_0 + R_0)$	r_{rh}	$=$	$\log(2)/15$
E_0	$=$	kC_0/p_d	p_d	$=$	0.2
I_0	$=$	kC_0/p_d	p_h	$=$	0.15
UD_0	$=$	$C_0(1/p_d - 1)p_{dth,0}$	r_v	$=$	0.5(new partial doses)$+0.95$(new
HD_0	$=$	$C_0 p_h p_{dth,0}$			complete doses)
QD_0	$=$	$C_0(1 - p_h)p_{dth,0}$	r_{re}	$=$	$\log(2)/1000$
UR_0	$=$	$C_0(1/p_d - 1)(1 - p_{dth,0})$	$p_{dth,0}$	$=$	$\Delta DD_1/(r_{dth}(DD_0 - p_d(R_0 + D_0)))$
HR_0	$=$	$C_0 p_h(1 - p_{dth,0})$			
QR_0	$=$	$C_0(1 - p_h)(1 - p_{dth,0})$			
V_0	$=$	0			
S_0	$=$	$N-$all other model states			

Note: Left column shows initial state values, in order of their derivation. k is calibrated to match the basic reproductive number of 6 - see explanation after equation 3.3. Right column shows calibrated parameter values, chosen to match epidemiological properties of the Covid-19 as well as data on vaccination and death.

vaccines were not available initially, and S_0 is the residual number of population. See Table 2 for a summary of initial state values.

Calibrating epidemiological parameters

Transition rates and probabilities $r_i, r_d, r_{dth}, r_{ri}, r_{rh}, p_d, p_h$ are calibrated to characteristics of the Covid-19, assuming these are constant and similar across economies (see also Li et al. (2020)). These are set in relation to the median time spent in the states, e.g. the incubation median time is about 5 days, which implies the incubation-to-infection daily transition probability $r_i = \log(2)/5$ (using a continuous-time approximation). The median virus detection time is 2 days, the median recovery time is 10 days, the median recovery time conditional on hospitalisation is longer at 15 days. The probability of being detected by tests p_d is set to 0.2 – for each confirmed case, there are 5 more who are undetected.[6] Those in quarantine who eventually succumb to the disease die on average after about one day and a half ($r_{dth} = 0.5$). Probability of hospitalisation conditional on being detected is 15%. The vaccination pace r_v is as described above, and the reinfection rate is rare with median person losing immunity after about 3 years. See Table 2 for a summary of parameter calibrations.

3.2   Fitting model to data

The model has three key unknowns: the initial state variables, the time-series of infection rate γ_t, and the time-series of death probability $p_{dth,t}$. Take each in turn.

   The sequences γ_t and $p_{dth,t}$ are reverse-engineered period by period from future observations using the model equations as restrictions. First, solve the observation equation

---

[6]One could argue that the detection probability depends on test intensity, making p_d time-varying. This is not considered here however.
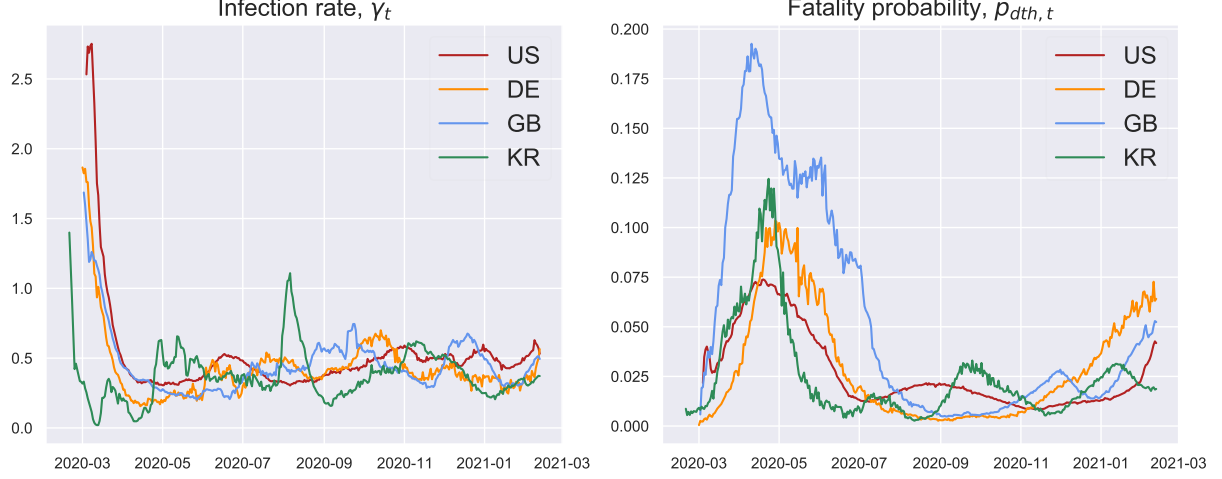
Note: Left panel shows the 7-day moving averages of the infection rates γ_t for selected countries, calculated using equation 3.3. Right panel shows the death probabilities $p_{dth,t}$ for the same set of countries, computed from equation 3.4.

Figure 3: Infection rate and fatality probability

3.1 (for ΔDT_t) backward using the dynamic equations to get:

$$\gamma_t = \frac{N}{r_i S_t I_t} \left[\frac{\Delta DT_{t+2}}{r_d p_d} - (1-r_d)^2 I_t - r_i(2 - r_d - r_i)E_t \right] \tag{3.3}$$

Recall that k determines E_0 and I_0 hence, according to equation 3.3, pins down the initial infection rate γ_0. Exploiting the fact that $\gamma_0 / r_d \equiv R0$, k is calibrated to produce the basic reproductive number $R0 = 6$ based on a study from Wuhan (see Sanche et al. (2020)).

I simulate the dynamic system 2.1-2.12 and concurrently filter out γ_t using equation 3.3 subject to a and a non-negativity constraint $\gamma_t > 0, \forall t$, using initial conditions S_0, I_0, E_0 and an end-point assumption $\Delta DT_{T+2} = \Delta DT_{T+1} = \Delta DT_T$, where T is the last in-sample period. This fast and robust algorithm recovers the entire time-series of γ_t as well as the model's latent state variables within the sample.

Similarly for $p_{dth,t}$, solving the observation equation 3.2 (for ΔDD_t) together with the dynamic equations 2.1-2.12 gives:

$$p_{dth,t} = \frac{\Delta DD_{t+1} - r_{dth}(1 - r_{dth})(HD_t + QD_t)}{r_{dth} r_d p_d I_t} \tag{3.4}$$

where $p_{dth,t}$ is restricted to be non-negative and assuming $\Delta DD_{T+1} = \Delta DD_T$. The result is the time-varying fatality probability consistent with fatality data and the model.

Figure 3 depicts γ_t and $p_{dth,t}$ for selected countries, whose fluctuations stem from a confluence of factors. The infection rate was highest at the initial stage of the pandemic, but declined sharply probably because social distancing and other restrictive measures came into effects. Death probability $p_{dth,t}$ was similarly higher early on in the pandemic, generally peaking in April at the height of the first wave when hospitals were most congested. The probability then declined substantially, in some cases approaching zero, as infections slowed and treatment improved. The second wave saw the death probability picking up again, though so far this remains much smaller than the 2020 peak.

3.3 Projections

Joint epidemiological-mobility projections entail forecasting γ_t and $p_{dth,t}$ (in addition to making assumptions about vaccination, deferred to the next section). Recall that γ_t depends in part on mobility, which endogenously evolves with the pandemic: $\gamma_t = \gamma_t^m + \gamma_t^d$ and $\gamma_t^m = \beta_0 \exp(\beta_1 m_t)$ (equation 2.14 and 2.15). To estimate how much mobility m_t affects the infection rate γ_t, one simple procedure is to optimise over β_0 and β_1 to minimise the mean-square prediction error:

$$\min_{\beta_0, \beta_1} \sum_{t=1}^{T} (\gamma_t - \beta_0 \exp(\beta_1 m_t))^2 \tag{3.5}$$

The resulting estimates $\hat{\beta}_0, \hat{\beta}_1$ imply the residual infection rate $\gamma_t^d \equiv \gamma_t - \hat{\gamma}_t^m$ for $t \leq T$, which has zero sample mean by construction. The autoregressive parameter ρ governing γ_t^d in equation 2.16 can then be estimated via a linear regression, which is then used to forecast γ_t^d for $t > T$. Intuitively, this formulation assumes that the effects impinging on the infection rate from all factors outside mobility dissipates in the future.

The society takes the estimates $\hat{\beta}_0, \hat{\beta}_1$ and γ_t^d as given when choosing the optimal mobility. The welfare weight ϕ on mobility is estimated for each country, by taking the latest observations $m_T, i_T, s_T, \tilde{\gamma}_T$ and backing out the implicit value of ϕ that satisfies the first-order condition 2.24 holds. That is, the society is assumed to choose mobility optimally in the last period, which reveals its preferences. The resulting policy function completes the forecasting procedure for γ_t

The evolution of death probability $p_{dth,t}$, as stated in equation 2.17, depends in part on how pervasive and targeted vaccinations are. Abstracting from these vaccine effects, it is assumed for simplicity that the underlying fatality probability follows a martingale:

$$\tilde{p}_{dth,t} = \tilde{p}_{dth,t-1} \tag{3.6}$$

Thus, any changes in the effective death probability $p_{dth,t}$ owe entirely to vaccination. This implies that, in the absence of reinfection, $p_{dth,t}$ is weakly decreasing with time. One justification for this assumption is that any progress made to reduce fatality rate through therapeutic procedures should be permanent if knowledge is not lost. At the same time, the assumption ignores other potentially important factors, such as the effects of ICU congestion, fatality rate associated with new virus strains, or the disease-mitigating (as opposed to disease-blocking) immunity developed by population over time. The current framework could be modified to accommodate these extensions however, assuming data are available to identify these effects.

4 Surviving the last lap: scenario analysis

This section presents the epidemiological-economic projections under various scenarios.

4.1 Baseline scenario: smooth pandexit

The baseline scenario assumes **steady progress in vaccinations**. Those that have started their inoculation campaign could continue vaccinating at a linear pace and deplete all contracted

dosages by end of 2021. For those that have contracted more dosages than entire population, any excess supply is assumed to translate into a faster vaccination roll-out.[7] As before, new daily effective vaccinations under this assumption are taken to be r_v in the model equation 2.12. The distribution of vaccines are assumed to be highly targeted, with $\eta = 0.8$ in equation 2.17. Reinfection continues to be extremely rare, with a median loss of immunity after roughly 3 years ($r_{re} = \log(2)/1000$).

Results

Figure 4 shows the simulation results for the United States as an illustration. In the top left panel, the total confirmed cases DT_t are projected to level off by the second quarter below 10% of total population, as the infectious population I_t continuing to fall. The stock of confirmed deaths on the top-right panel reaches its peak at less than 0.175% of population. The two panels also show how closely the filtered series DT_t and DD_t match the data on confirmed cases and deaths respectively within the sample.

Relatively quick stabilisation of cases and deaths owe mainly to the effects of vaccination - shown in the centre-left panel. Under the assumed roll-out pace, all remaining susceptible population should be inoculated by the second quarter. For the United States, the model estimates that 40% of population had already been exposed to the virus by the time vaccination programme began. This means only 60% of population need to be vaccinated to reach the point of absolute herd immunity.

Support from vaccinations during the 'last lap' of the pandemic allows some easing of restrictions immediately, with mobility projected to gradually return to its normal level in the second quarter. Also tilting the cost and benefit in favour of opening up is the falling death probability as a result of prioritising the elderly in the vaccination campaign. The bottom-right panel shows the projected fatality rate in thick black line, projected to decline by about half a percentage point in the coming months. The panel also shows the two counterfactual corner cases where vaccines were distributed randomly and in perfectly targeted way, showing the potential gain from vaccine distribution given the United States' demographic profile.

The model also produces a decomposition of the infection rate, providing a description of the past as well as the outlook. The centre-right panel shows the filtered infection rate γ_t (red line) and its two constituents, the contribution from mobility γ_t^m (blue line) and the exogenous term γ_t^d (orange line). Initially, the infection rate was very high both because of normal human mobility γ_t^m, as well as the lack of health precautions and the absence of social distancing which likely contributed to γ_t^d. Both components plunged substantially as society responded to the pandemic. Then the second wave caused another surge in infections around the fall of 2020, which the model largely attributed to the exogenous component γ_t^d. Looking ahead, the reopening of the economy would likely increase the infection rate again, though the effect on cases and deaths would be more muted given the protection from vaccination. In assuming stable γ_t^d, this projection also assumes persistent uses of masks and other health precautions during the forecasting period.

---

[7]Contracting multiple vaccines lowers the chance of being constrained by a single producer's supply bottleneck, which is one reason why some countries secure more dosages than needed and establish arrangements with more than one producer.
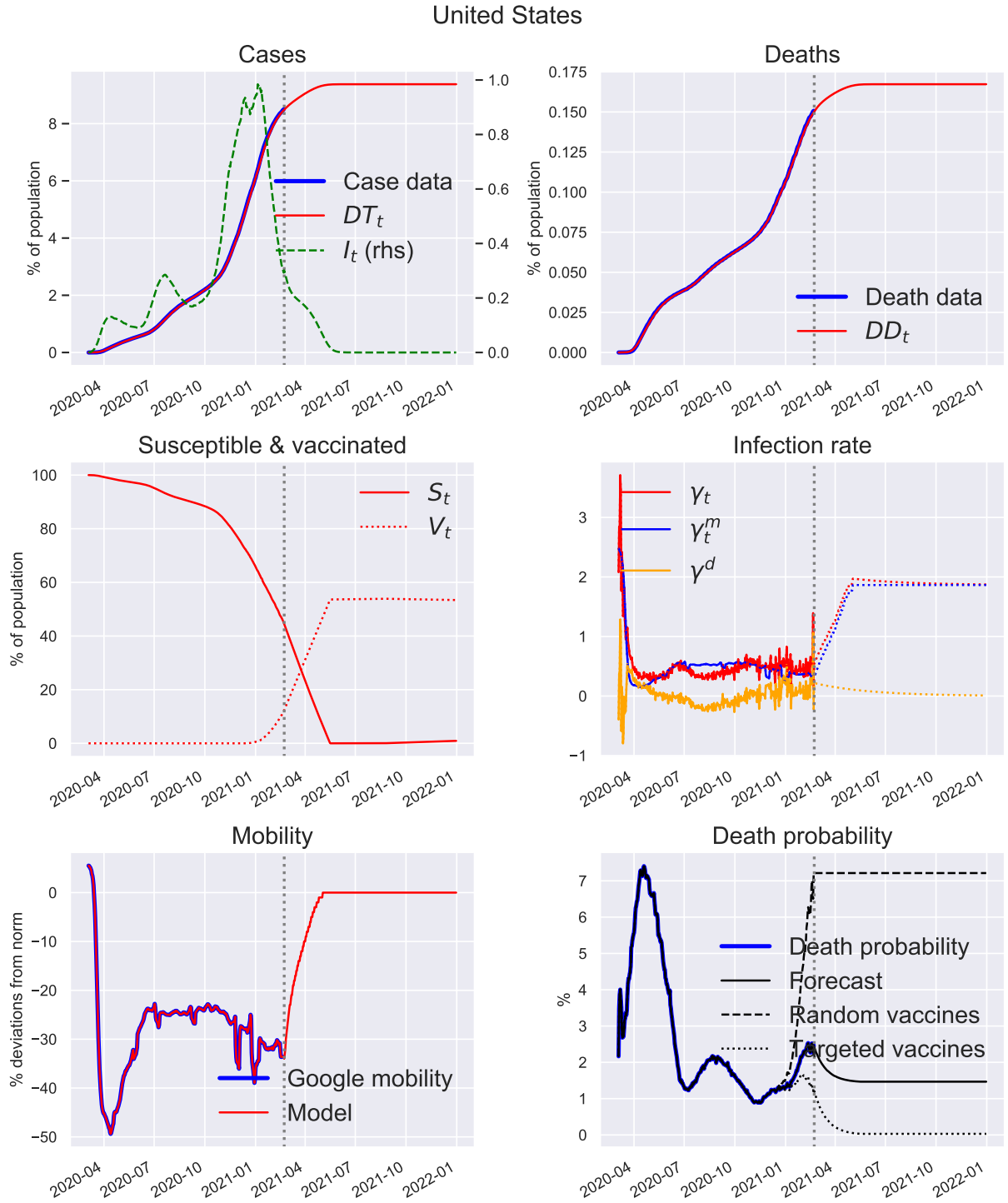
Note: Baseline projections of key epidemiological states and mobility. Assumes steady vaccinations at a pace that will deplete all contracted dosages by end of 2021.

Figure 4: Baseline projections for United States
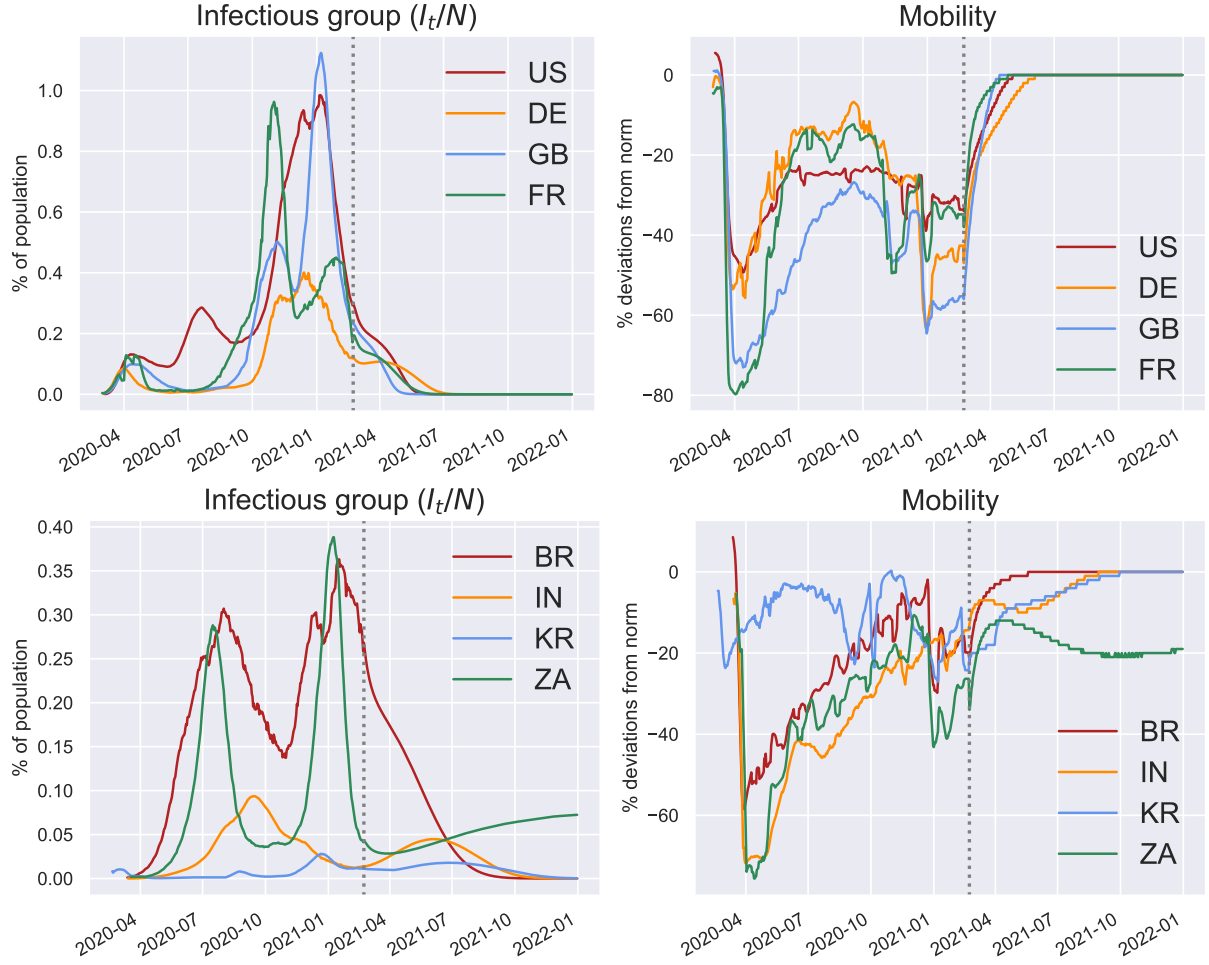
Note: Baseline projections of infectious states and mobility. Assumes steady vaccinations at a pace that will deplete all contracted dosages by end of 2021.

Figure 5: Baseline projections for selected economies

Other advanced economies that are ramping up vaccinations share similarly benign outlook. Figure 5 compares the projections for infectious population I_t on the left column and implied mobility choices on the right, for selected group of economies. The top row features major advanced economies including France, Germany and United Kingdom together with the United States. Infectious population should steadily decline in these economies, approaching zero by the first half of the year allow them to open up. Among this group, mobility restrictions are needed the longest in Germany, as comparatively few infections to date mean a larger susceptible population at risk. For a given pace of vaccination, it thus takes longer to fully protect the entire population. But even in this case, mobility could return to normal by the second quarter.

Outlook for emerging market economies (EMEs) is more heterogeneous, due to different progress in vaccinations as well as societies' varied responses to the pandemic developments. The bottom row of Figure 5 shows the simulation results for selected EMEs. Brazil has a relatively high share of infectious population, but vaccination has already started and if the roll-out goes ahead as assumed, infections should continuously drop. Estimated weight on maintaining economic activity ϕ is also relatively high, supporting a quick resumption of

mobility as infections moderate. By contrast, Korea has fewer infections, but a higher weight on health objective, a very high share of susceptible population and a later start of vaccination imply a slower recovery of mobility. In South Africa, a combination of very high death rate and assumed pace of vaccination suggests mobility restrictions may continue to be necessary.

4.2   3rd wave scenario

In this '3rd wave' scenario, the infection rate jumps temporarily for factors unrelated to mobility. Reasons could be an importation of a new strain from another country, which could subsequently be suppressed and eradicated it becomes endemic domestically. To implement the scenario, γ_t^d is subject to positive shocks for 10 consecutive days, before gradually mean-reverting to zero according to its autoregressive process. Other assumptions are the same as under baseline.

Results

A positive shock to the infection rate gives rise to a greater need for mobility restrictions relative to the baseline. This scenario exposes in particular those that are vaccinating more slowly. Figure 6 examines possible implications of a 3rd-wave shock using Germany and Brazil respectively, as examples. In Germany, an infection rate spike triggers more cases and prompts another round of mobility restrictions. This measure would restrain the overall infection rate (left panel), and allow for a reopening which is postponed to the second quarter. In Brazil, the infection rate spike could justify a particularly sharp reduction in mobility, as vaccination has yet to reach a large part of population. Another reason is that the estimated sensitivity of infection rate to mobility is lower in Brazil than in Germany, which means it takes sustained mobility restrictions to contain the outbreak. In the left panel of Figure 6, γ_t under this scenario stays higher than the baseline despite large reduction in mobility.

4.3   Slower vaccination scenario

In this scenario, vaccination proceeds at a third of the baseline pace. Those that have not started vaccination are assumed to push back the starting date from end of March to end of June. Reasons could be related to supply, such as slow production or logistical obstacles, or demand if part of population elect not to receive injections due to safety concerns.[8]   Other assumptions are identical to baseline.

Results

Vaccination hiccups tend to be more disruptive in countries which have to inoculate a large swath of population to obtain herd immunity and are vaccinating at a relatively slow pace to begin with. Figure 7 contrasts the outcomes of this scenario for the United States and India. In the first case, as mentioned earlier, less than 60% of population need full dosages to reach complete immunity and the baseline case assumes that this could be done within the first half of the year. Delay in vaccination pushes the point of immunity towards the end of the year, which

---

[8]According to Ipsos survey taken in January 2021, as many as 30 percent of population in 15 countries surveyed express reluctance to receive vaccines even if they are available. See Ipsos (2021).
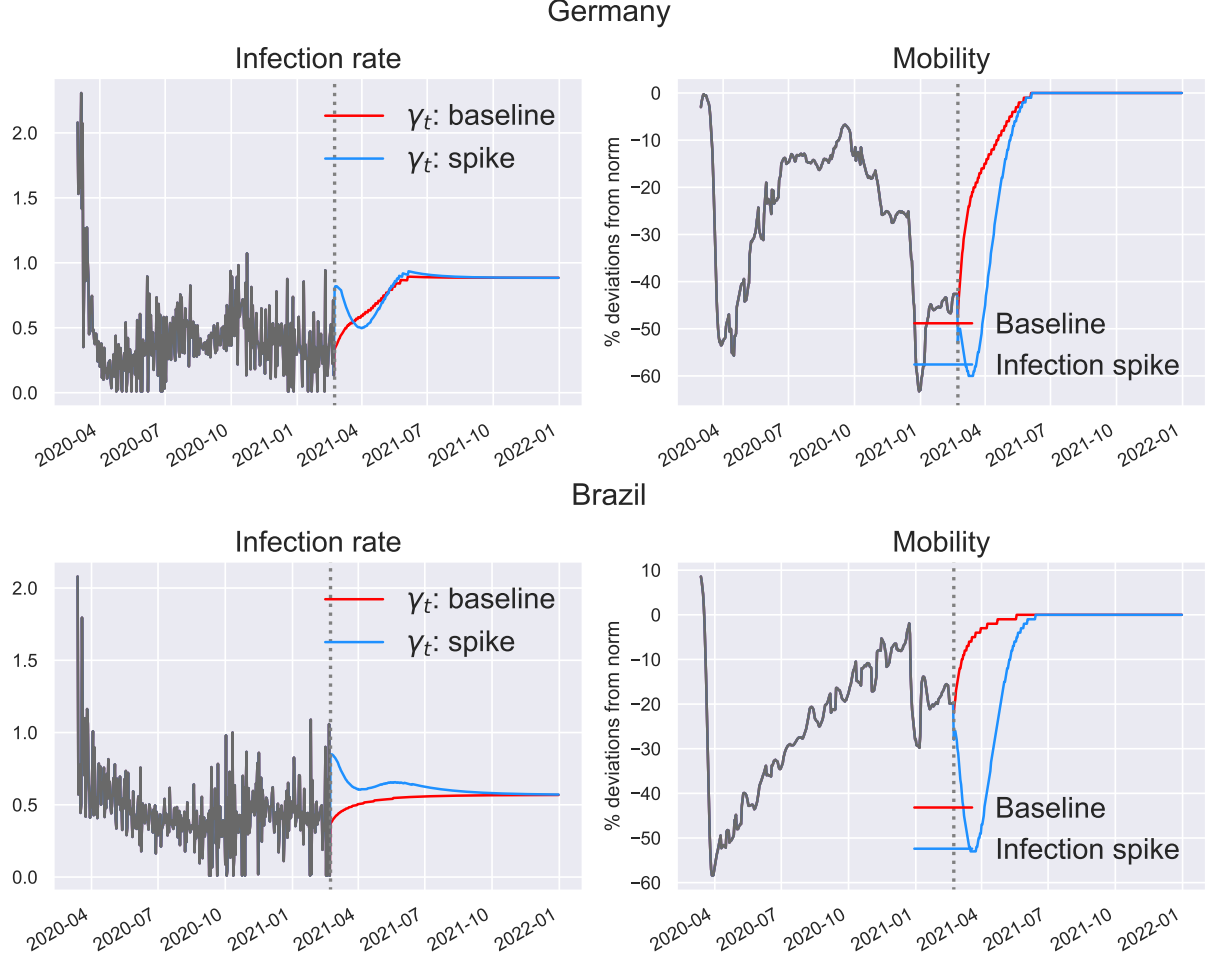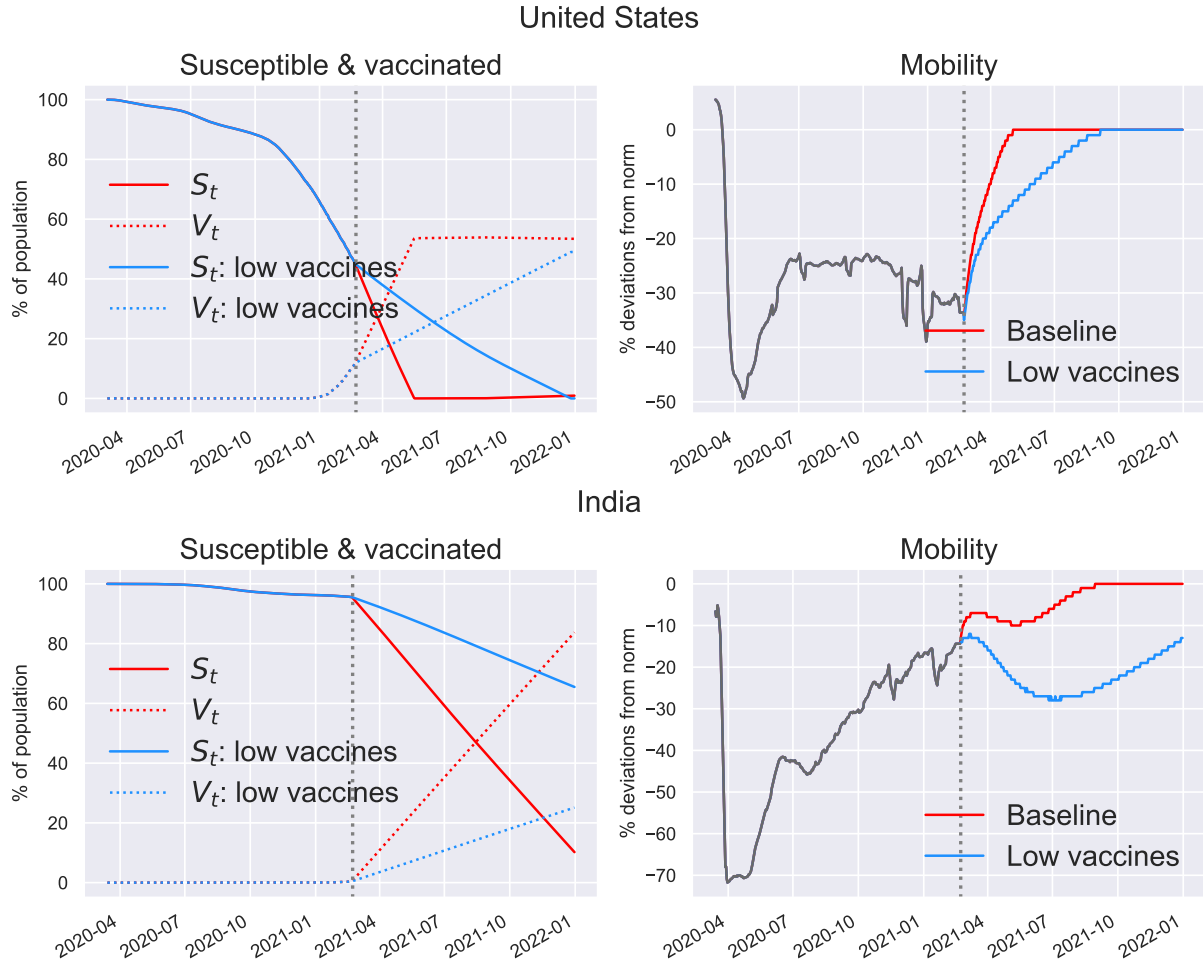
Germany

Note: Projections of susceptible and vaccinated population, as well as mobility. Baseline and a '3rd wave' scenario where the infection rate surges temporarily. Vaccination on track as in baseline.

Figure 6: 3rd wave: Germany and Brazil

justify some tightening in mobility restrictions in the interim period. Even so, mobility should normalise by the 3rd quarter, as only few susceptible individuals should remain. In India by contrast, the slower vaccination scenario implies over 60% of population will remain susceptible to the virus at the end of 2021. There is hence greater need for restricting mobility substantially below the baseline for the entire year, as the lower-right panel shows.

4.4 Reinfection scenario

This scenario entails a pervasive loss of immunity by those who have previously recovered from Covid-19 as well as those who have been effectively vaccinated. I assume a median immunity loss after 60 days, so that $r_r e = \log(2)/60$. This implies that about 1 percent of immune people become susceptible to the disease again each day. A primary reason for reinfection would be virus mutations. I assume continuous adaptation of both vaccines and the virus such that new injections still work in preventing infection (as vaccines are tweaked to deal with new strains) but the immunity is short-lived as the virus also continues mutating. However, the total vaccine supply and the roll-out pace is kept the same as under baseline.

16

Note: Projections of susceptible and vaccinated population, as well as mobility. Baseline against a slower vaccination scenario.

Figure 7: Slower vaccination: United States and India

Results

There is a race between virus mutations and vaccination in this scenario, with advantages going to the fastest to adapt and the one with most 'ammunition'. The scenario intentionally stacks the odds in favour of virus mutations, by assuming quite rapid reinfection rate and holding vaccine supply fixed – hence limited ammunition for vaccines. Figure 8 shows what could happen, using Germany and United Kingdom as illustrations. Initially, vaccination dominates and the pool of susceptible people shrinks, though at a slower pace than the baseline due to the reinfection headwind. But as vaccine supply is eventually depleted, reinfection starts to increase the susceptible pool. At this point, lockdowns become the only tool for slowing infections. In the simulations, the United Kingdom who is making faster progress in vaccination, is paradoxically the one that has to tighten activity more later on, as it will be without vaccine doses sooner.

4.5 Output impact of various scenarios

Using the mobility-output conversion factors explained in section 3.1, the implications of above scenarios for GDP are computed for the full set of countries and summarised in Figure 9. Under the baseline scenario, the median output loss for 2021 relative to no-pandemic benchmark is
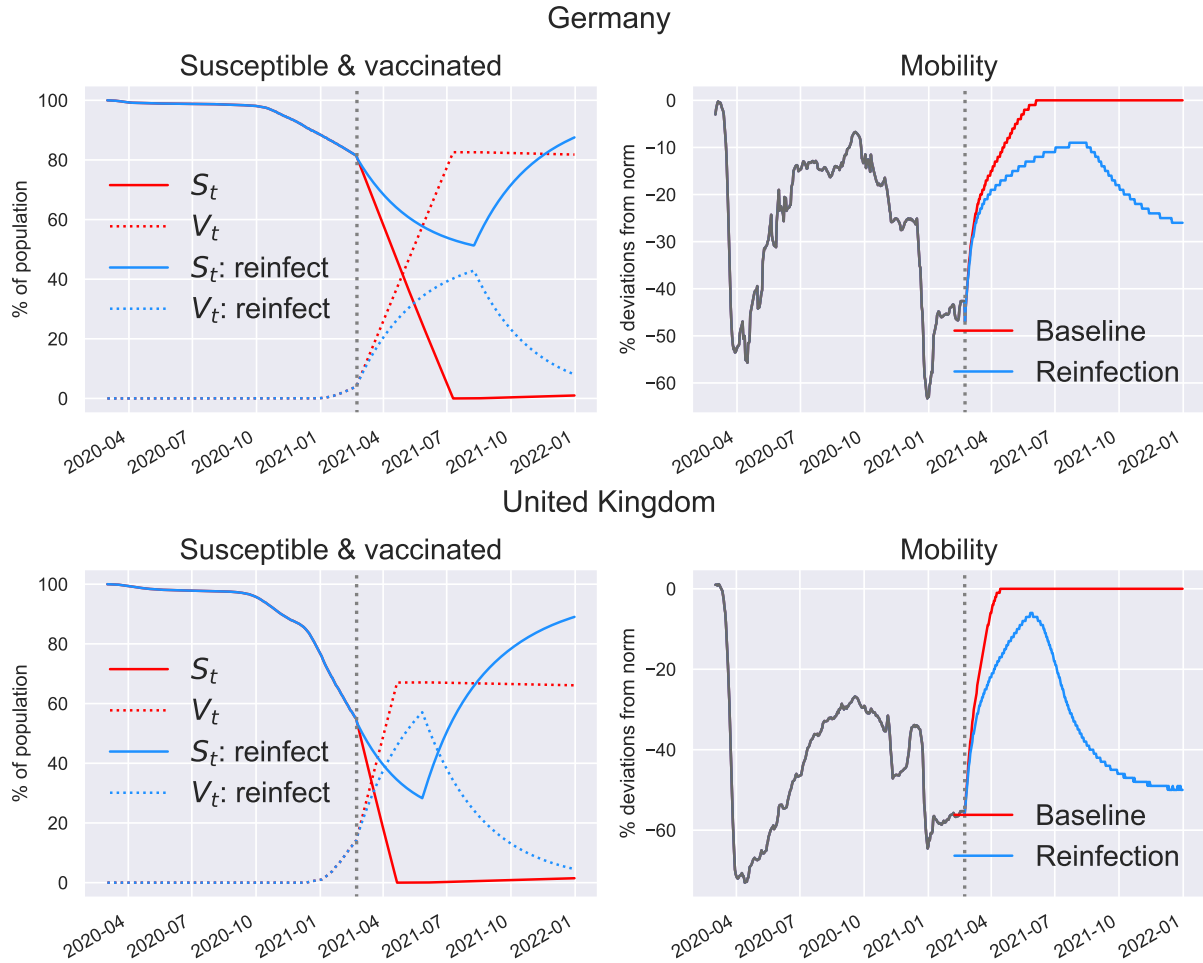
Note: Projections of susceptible and vaccinated population, as well as mobility. Baseline against a reinfection scenario.

Figure 8: Reinfection: Germany and United Kingdom

about 2.25 percentage points, much smaller than the corresponding loss in the previous year which is close to 8%. A temporary infection rate spike and slower vaccination scenarios are similarly costly, equivalent to about 3.75-4 percentage points median output losses for 2021. Perhaps unsurprisingly, the reinfection scenario is the most costly, entailing 5.75 percentage points of GDP forgone. The total economic costs could be much larger still, as it means the pandemic is not yet under control by the end of this year.

As discussed in the previous section, certain countries are more exposed to some scenarios than others. Advanced economies that are making good progress with vaccinations are naturally less vulnerable to a 3rd-wave shock. Indeed, the protection conferred by vaccines is why many of them could soon lift restrictive measures even if this would raise the infection rate. For some EMEs without such protection, a 3rd wave could be the most disruptive scenario at least in the short term.
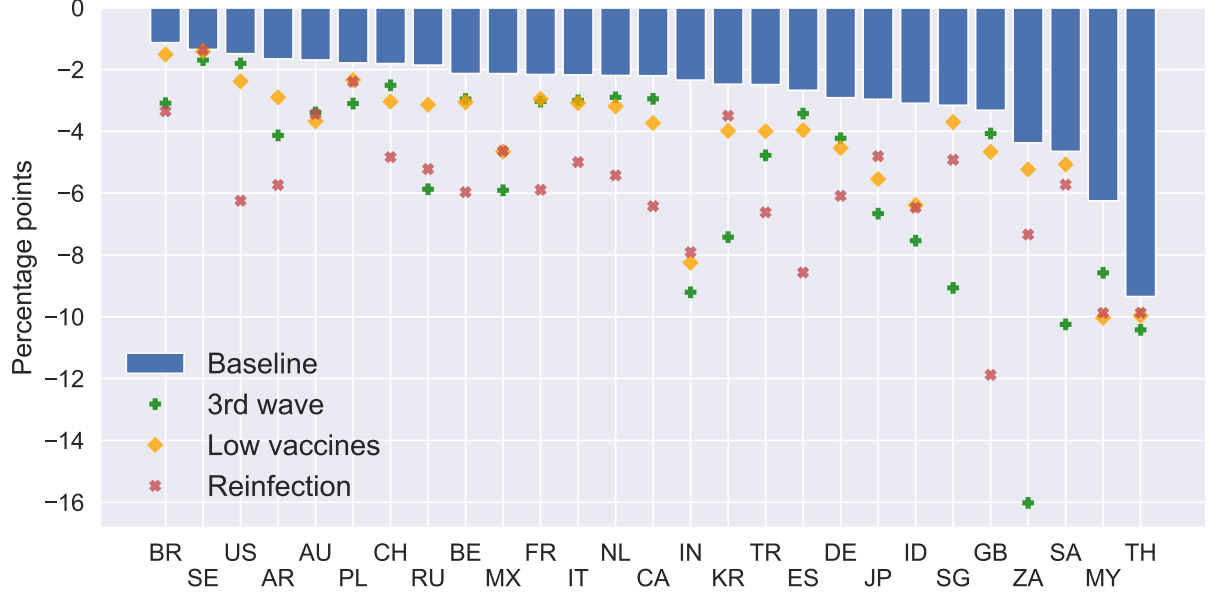
Note: Output losses for 2021 relative to no-pandemic benchmark, implied by the model's mobility forecasts times country-specific conversion factors.

Figure 9: 2021 output losses

5 Conclusion

The end of the pandemic may be within sight with the arrival of vaccines. But unexpected challenges could still emerge that complicate the pandexit process. This paper provides quantify the output implications of some downside scenarios that could transpire in the coming months. The substantial implications for output under these scenarios highlight the need for continued vigilance, and to speed up the roll-out of vaccines particularly in countries where susceptible population remains high.

Clearly the projections and scenarios presented are not exhaustive. One advantage of the framework is its flexibility, which allows it to easily accommodate various extensions, alternative assumptions and other scenarios. Detailed country-level information, e.g. regarding specific vaccines used or preferred vaccine distribution strategy, can be easily introduced. More substantial extensions are also possible. For instance, the mapping between mobility and output could be enriched to take account of potential nonlinearity, e.g. arising from insolvency and balance sheet amplifications. The closed-system construction is typical for an SEIR-type model, but the international spillovers could still be introduced in a reduced-form, e.g. by letting the infection rate γ_t be correlated across economies. Indeed, this may be where future challenges lie, given the uneven progress in vaccination which raises the prospect of the Covid-19 becoming endemic.

References

IPSOS (2021): "Global attitudes : Covid-19 vaccines," Ipsos survery for the world economic forum.

LI, M. L., H. T. BOUARDI, O. S. LAMI, N. TRICHAKIS, T. TRIKALINOS, M. F. ZARANDI, AND D. BERTSIMAS (2020): "Forecasting COVID-19 and Analyzing the Effect of Government Interventions," mimio.

O'DRISCOLL, M., G. RIBEIRO DOS SANTOS, L. WANG, D. A. T. CUMMINGS, A. S. AZMAN, J. PAIREAU, A. FONTANET, S. CAUCHEMEZ, AND H. SALJE (2020): "Age-specific mortality and immunity patterns of SARS-CoV-2," *Nature*.

POLACK, F. P., S. J. THOMAS, N. KITCHIN, J. ABSALON, A. GURTMAN, S. LOCKHART, J. L. PEREZ, G. PÉREZ MARC, E. D. MOREIRA, C. ZERBINI, R. BAILEY, K. A. SWANSON, S. ROYCHOUDHURY, K. KOURY, P. LI, W. V. KALINA, D. COOPER, R. W. FRENCK, L. L. HAMMITT, TÜRECI, H. NELL, A. SCHAEFER, S. ÜNAL, D. B. TRESNAN, S. MATHER, P. R. DORMITZER, U. ŞAHIN, K. U. JANSEN, AND W. C. GRUBER (2020): "Safety and Efficacy of the BNT162b2 mRNA Covid-19 Vaccine," *New England Journal of Medicine*, 383, 2603–2615.

RUNGCHAROENKITKUL, P. (2021): "Macroeconomic effects of Covid-19: a mid-term review," mimio.

SANCHE, S., Y. T. LIN, C. XU, E. ROMERO-SEVERSON, N. HENGARTNER, AND R. KE (2020): "High contagiousness and rapid spread of severe acute respiratory syndrome coronavirus 2," *Emerging Infectious Diseases*, 26.

Appendix A   Baseline simulations

This appendix presents the full baseline simulation results for remaining 26 countries, in addition to Figure 4 which shows the result for the United States. For simulation under alternative scenarios, see the chart pack in https://github.com/phurichai/covid19macro.
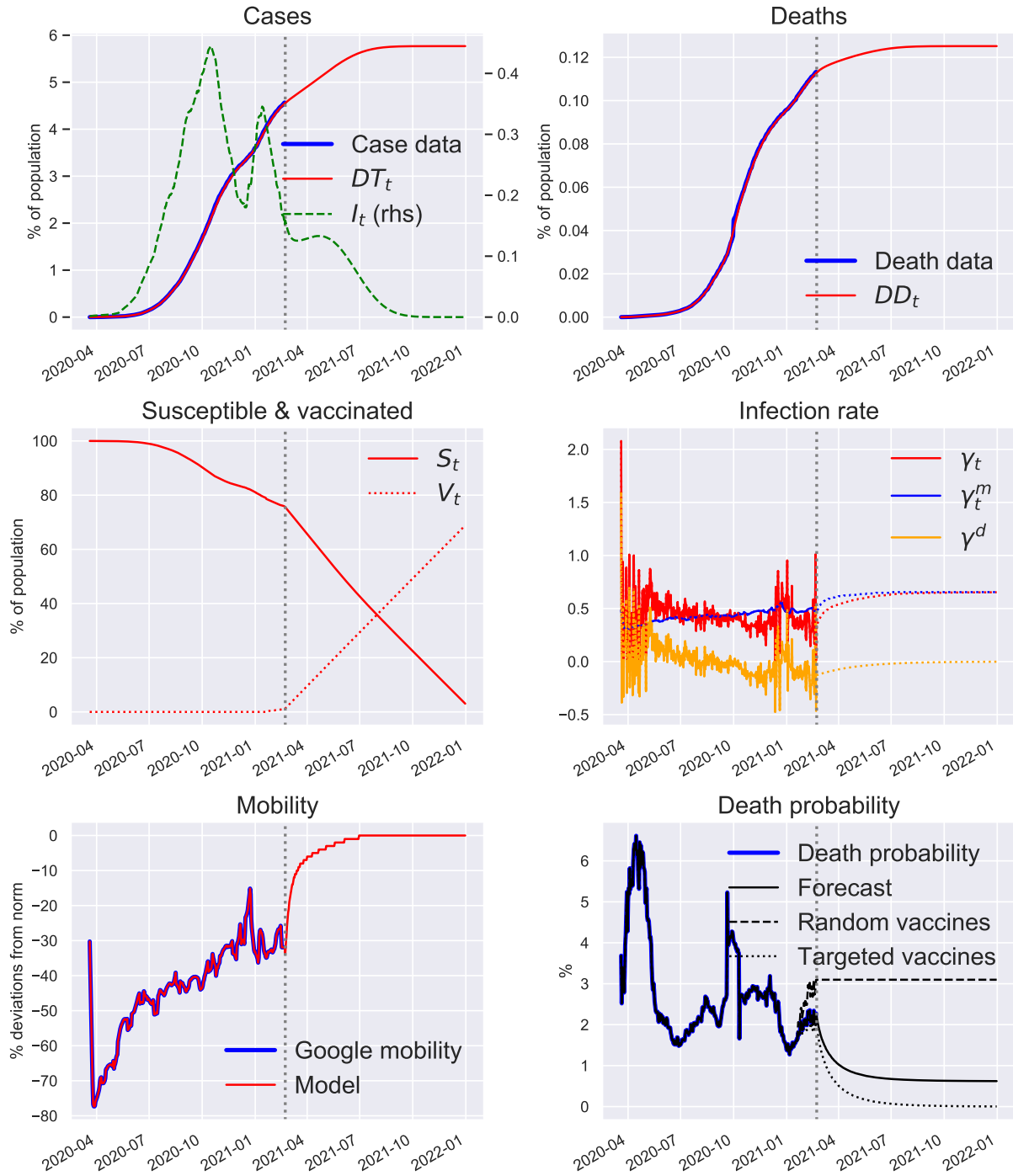
Argentina

Cases

Deaths

Susceptible & vaccinated

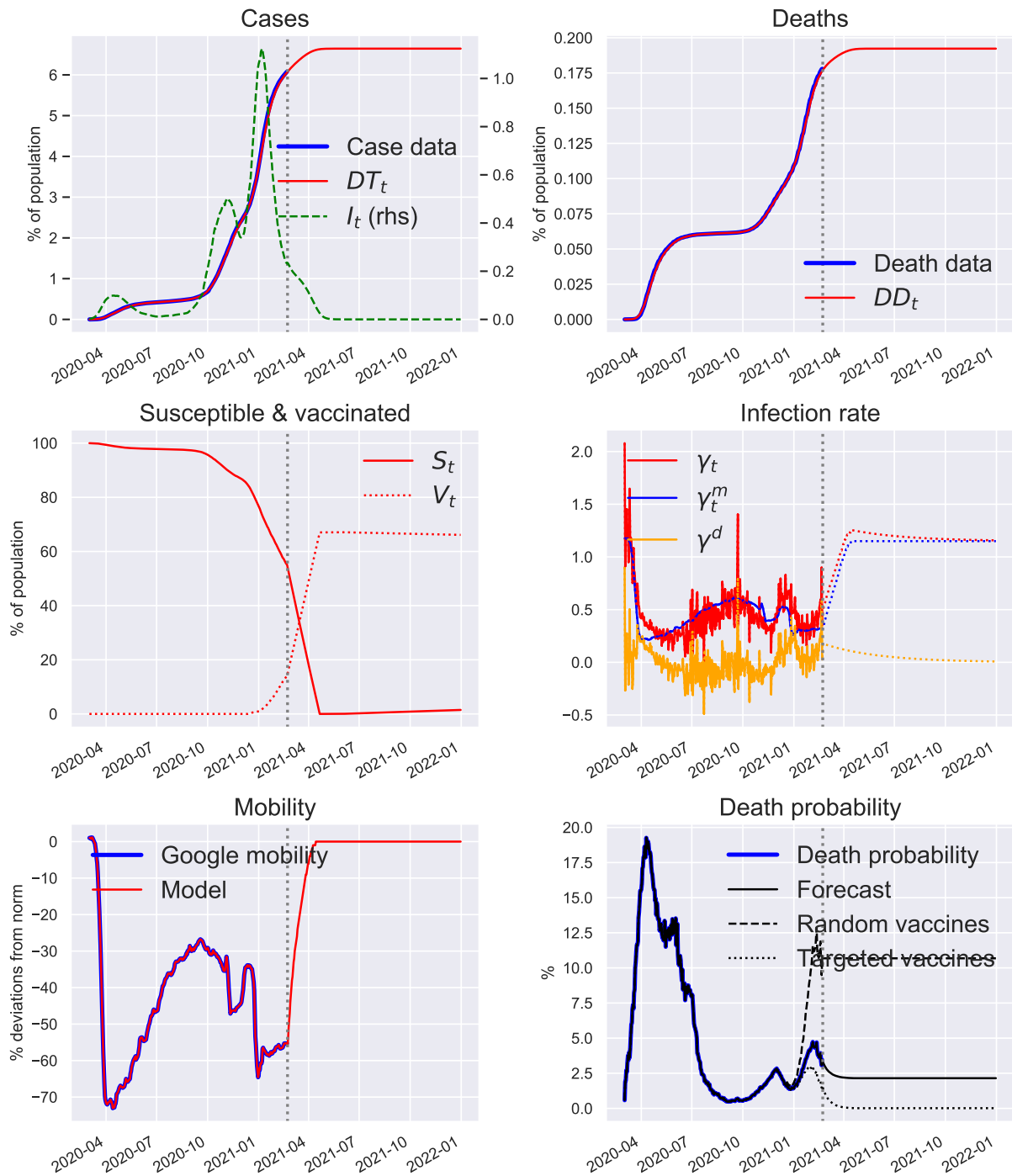## Infection rate
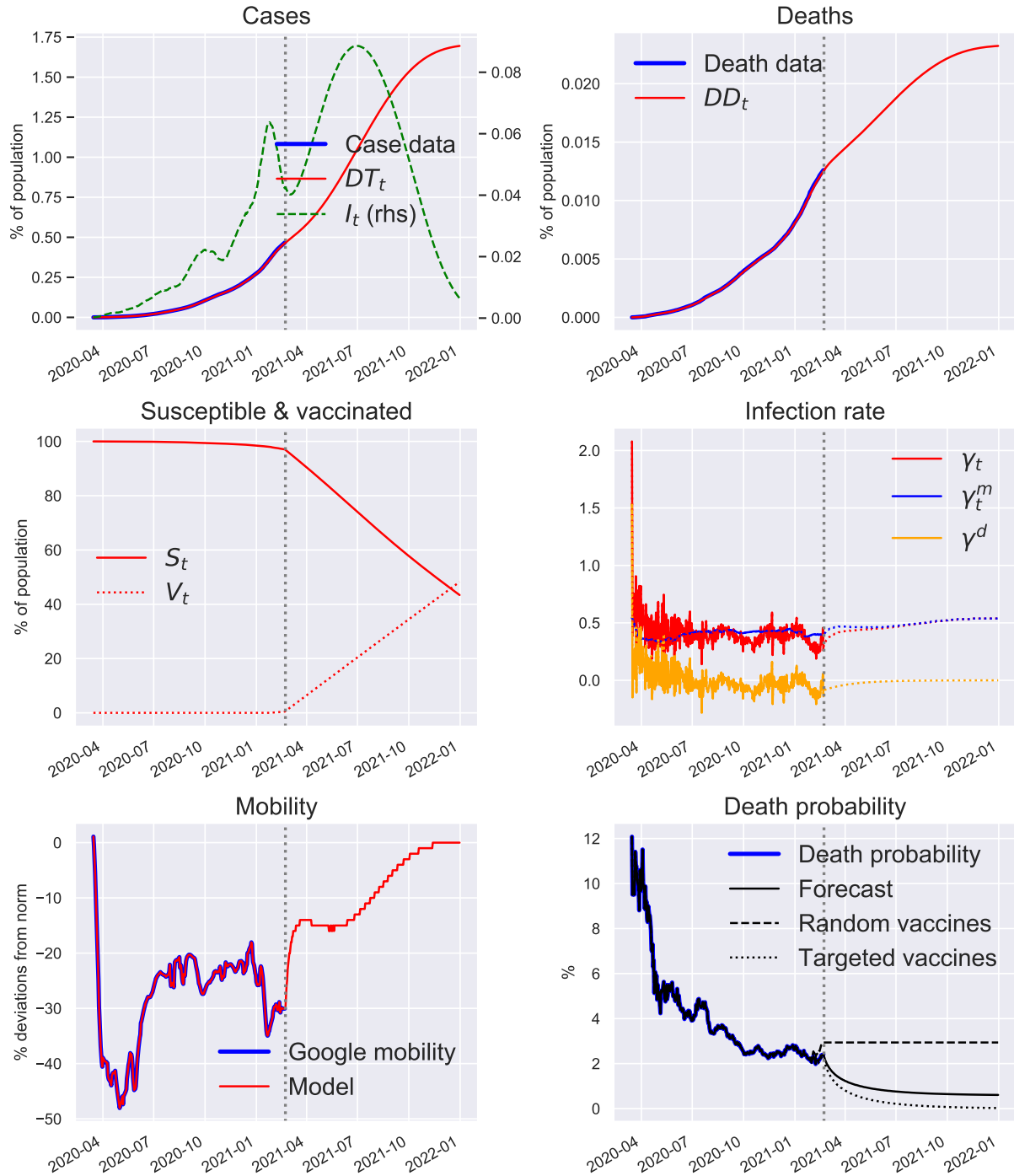

Mobility

Death probability

Note: Baseline projections of key epidemiological states and mobility. Assumes steady vaccinations at a pace that will deplete all contracted dosages by end of 2021.

Australia
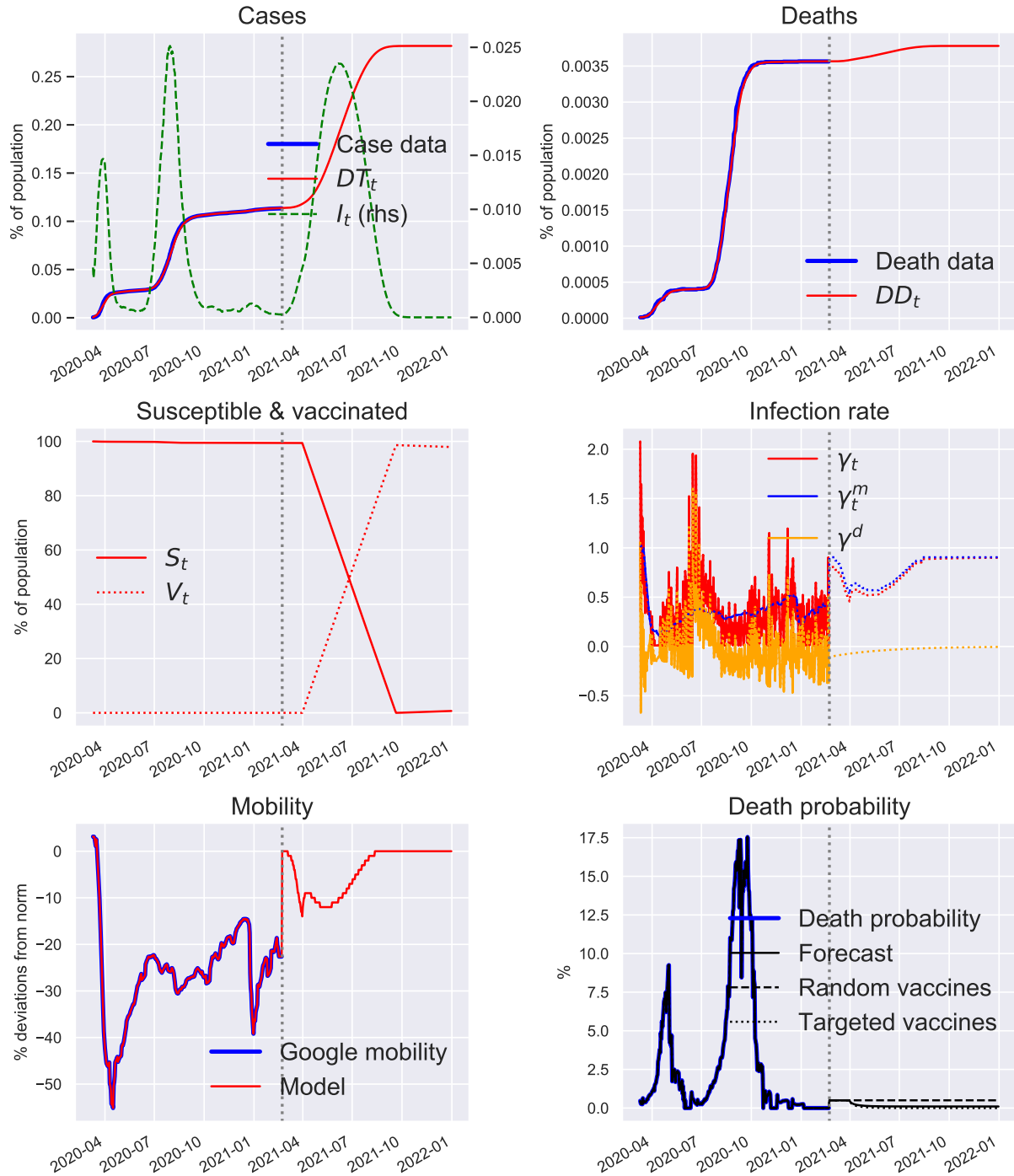
Note: Baseline projections of key epidemiological states and mobility. Assumes steady vaccinations at a pace that will deplete all contracted dosages by end of 2021.

Belgium
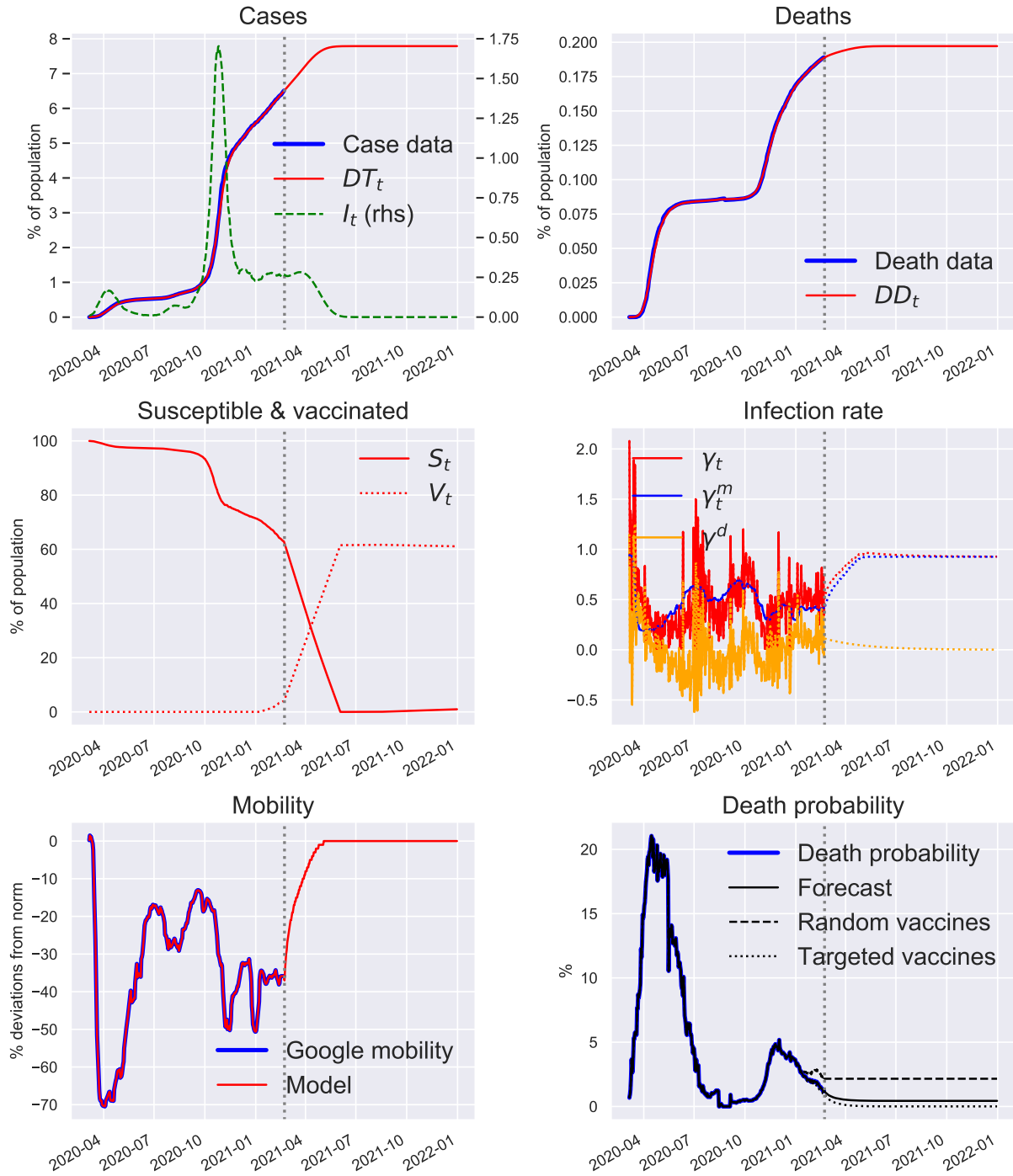
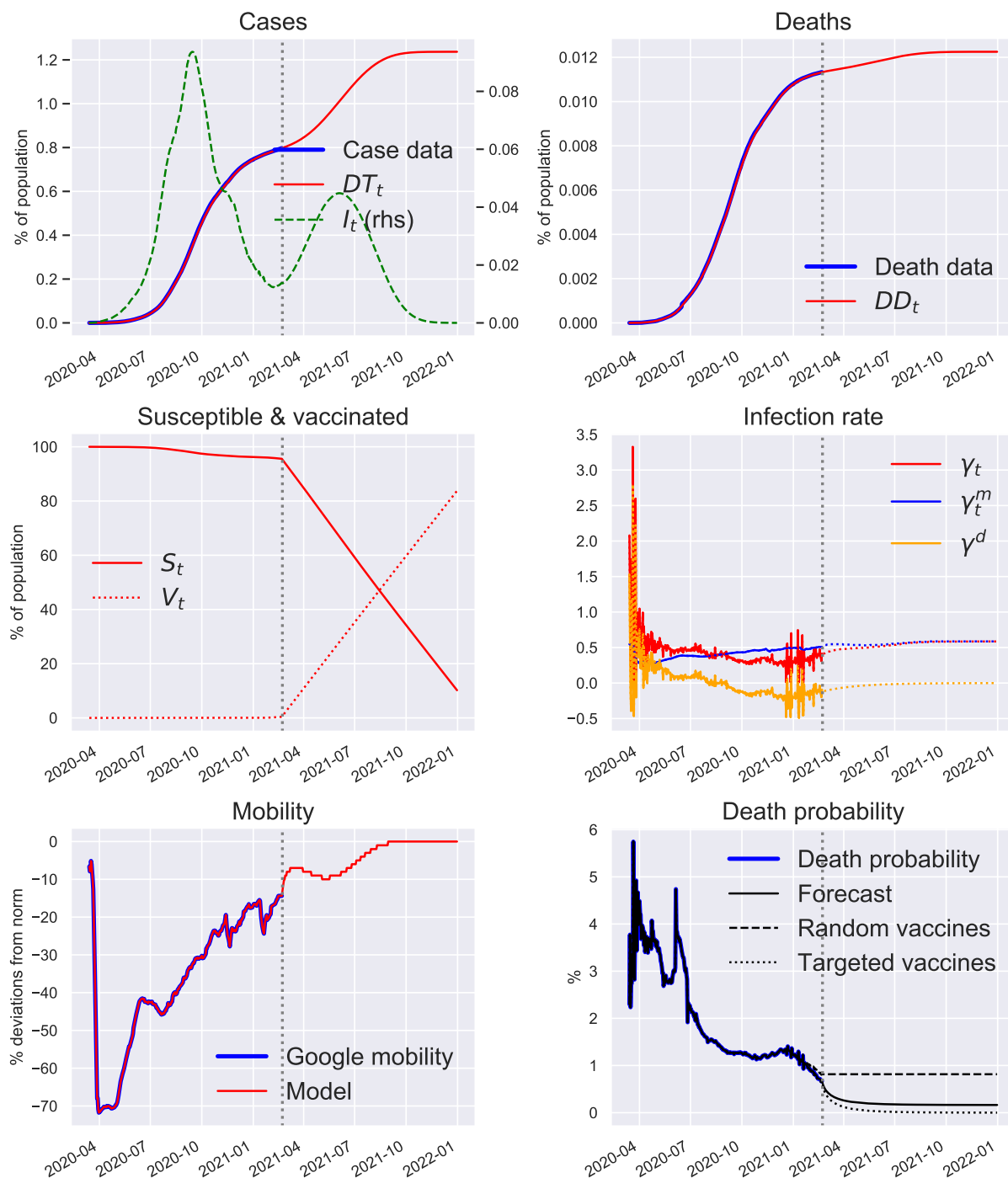**Note**: Baseline projections of key epidemiological states and mobility. Assumes steady vaccinations at a pace that will deplete all contracted dosages by end of 2021.

Brazil
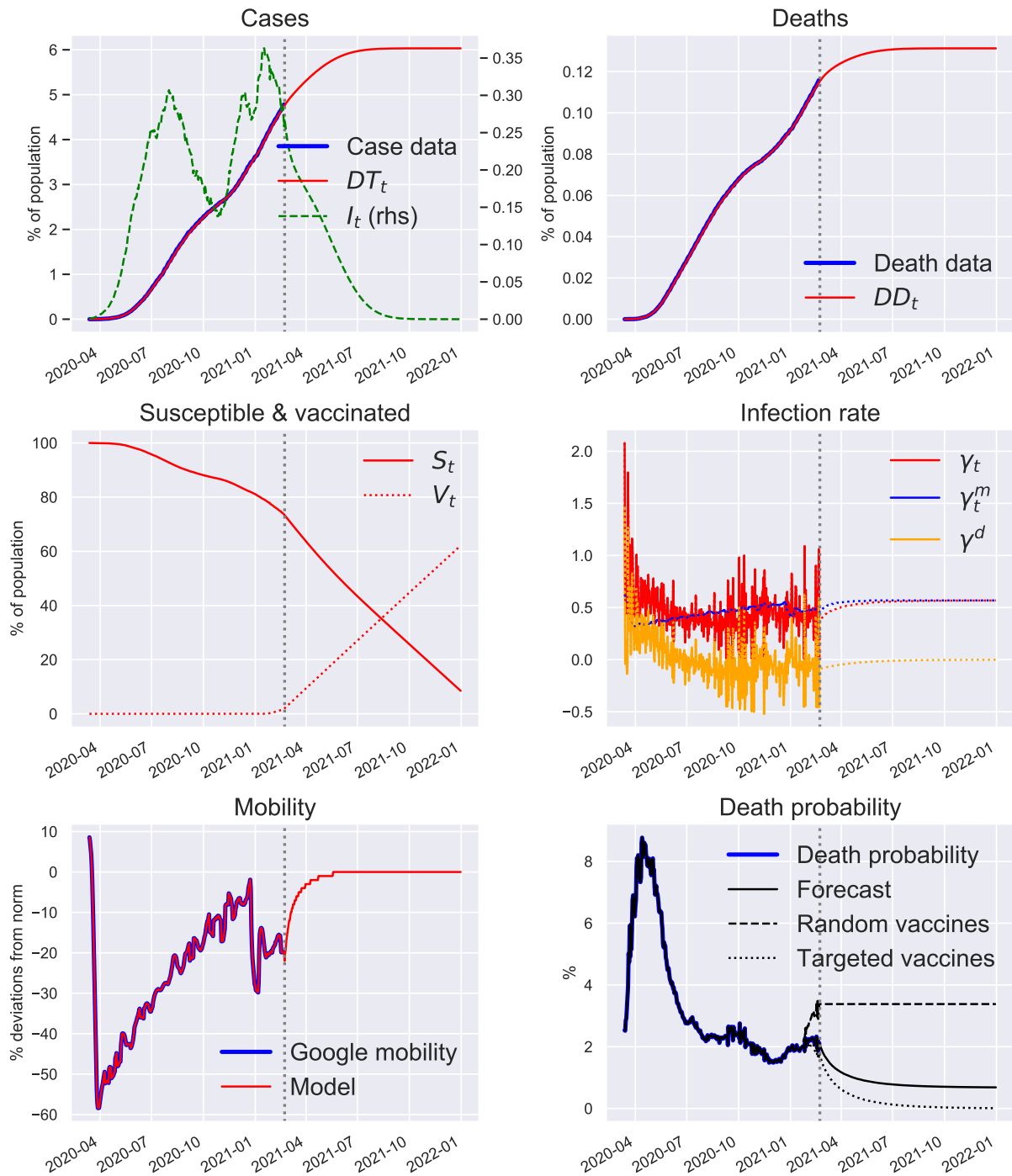
Note: Baseline projections of key epidemiological states and mobility. Assumes steady vaccinations at a pace that will deplete all contracted dosages by end of 2021.
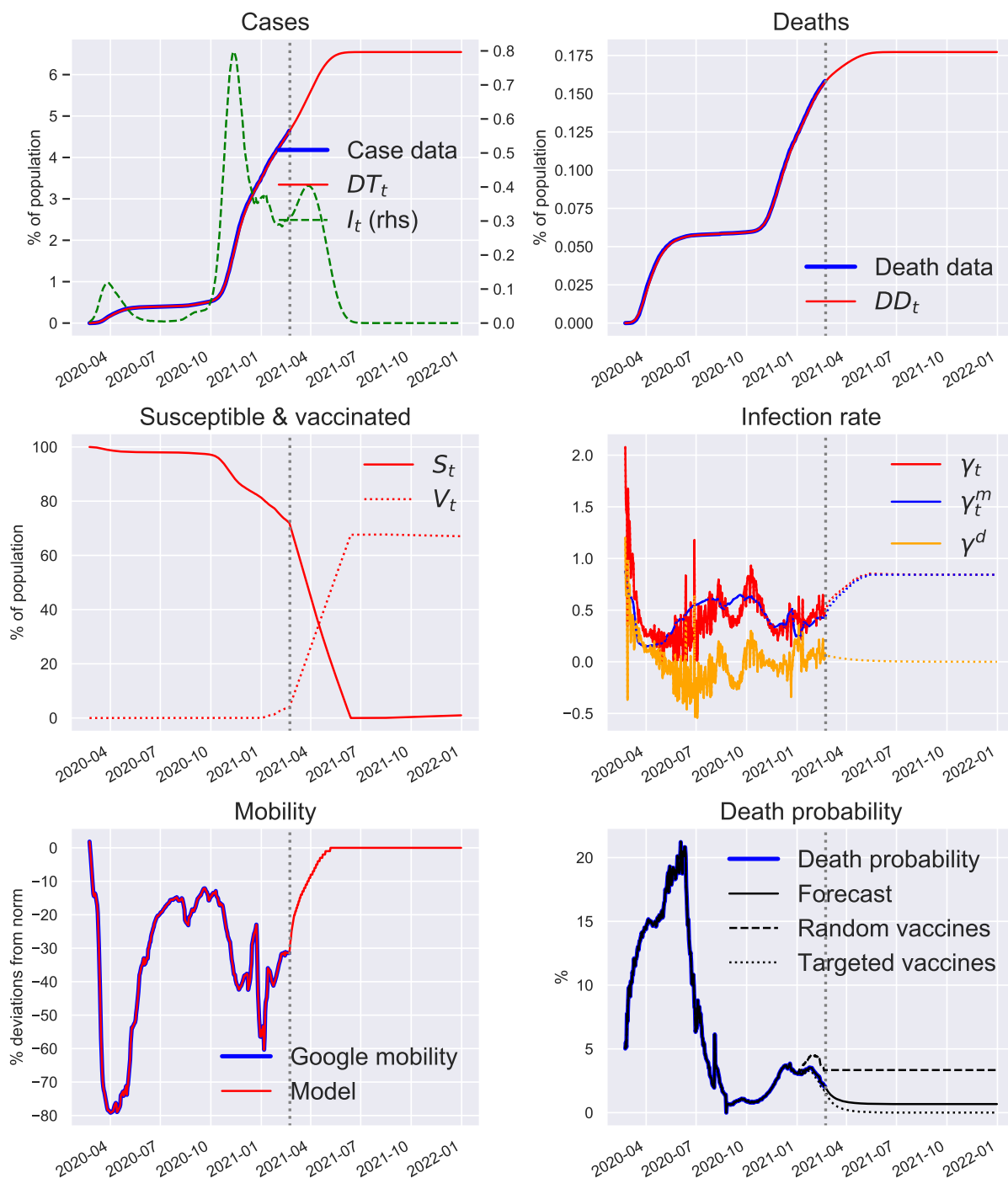
Canada
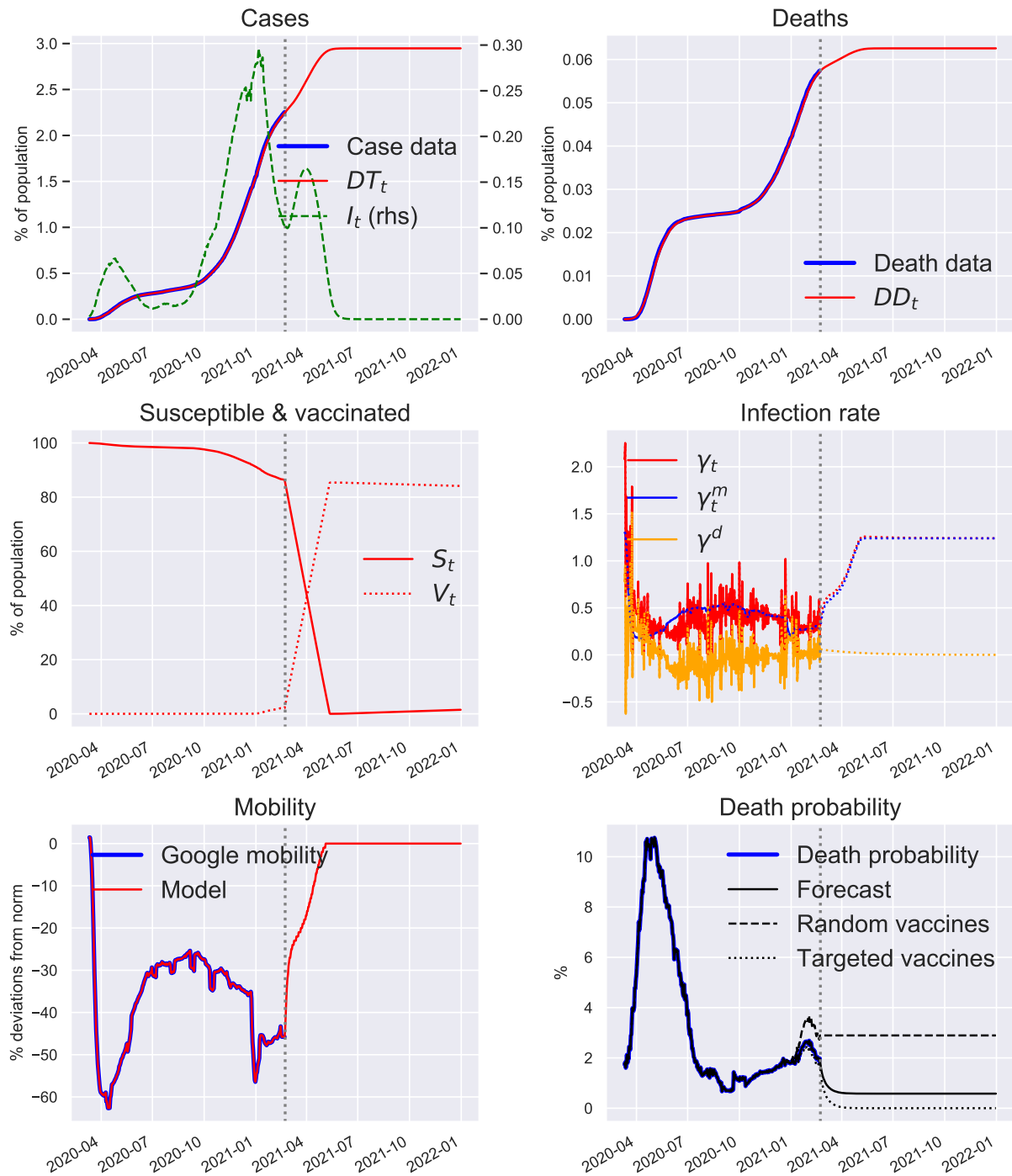
Note: Baseline projections of key epidemiological states and mobility. Assumes steady vaccinations at a pace that will deplete all contracted dosages by end of 2021.
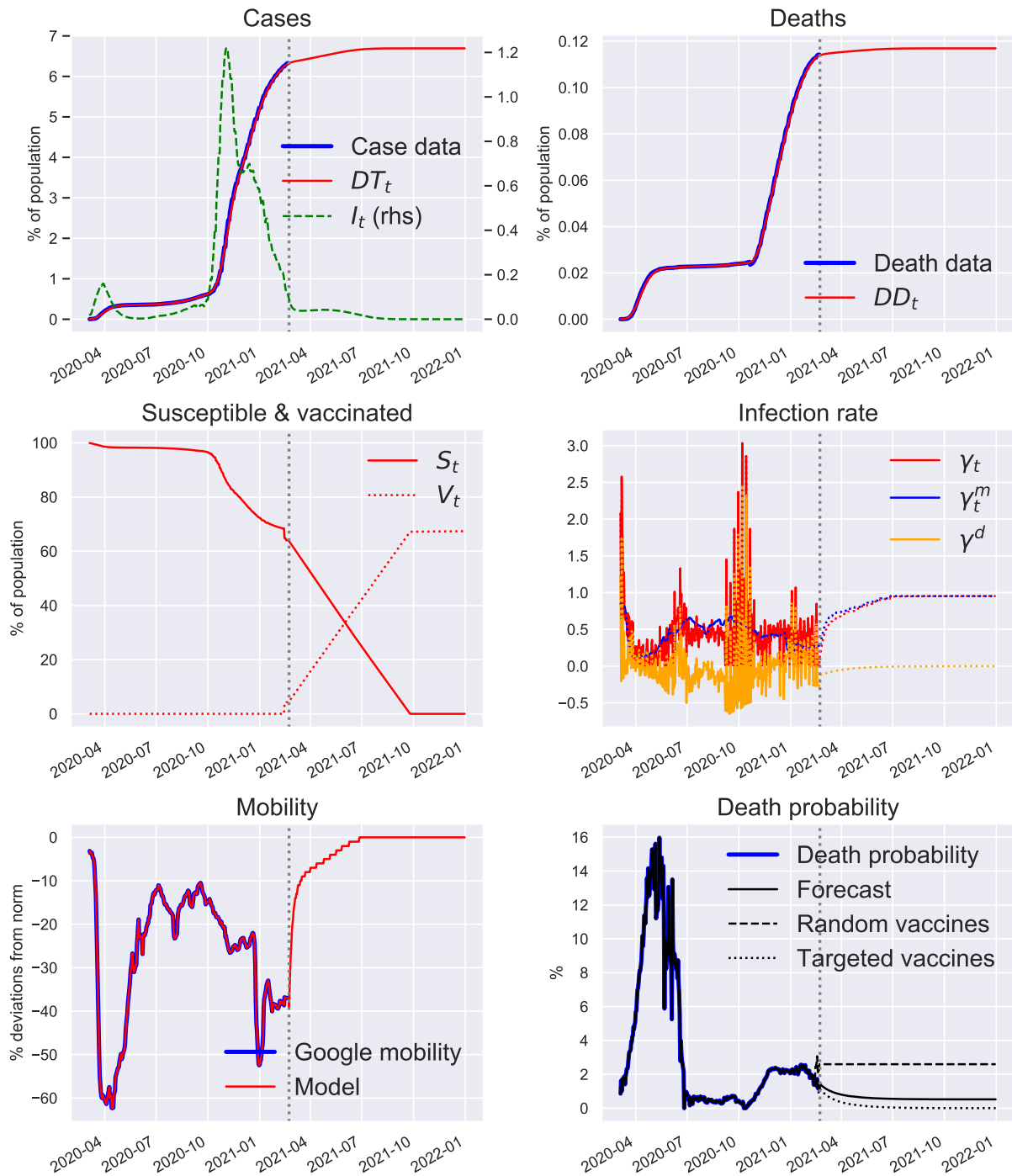
Note: Baseline projections of key epidemiological states and mobility. Assumes steady vaccinations at a pace that will deplete all contracted dosages by end of 2021.
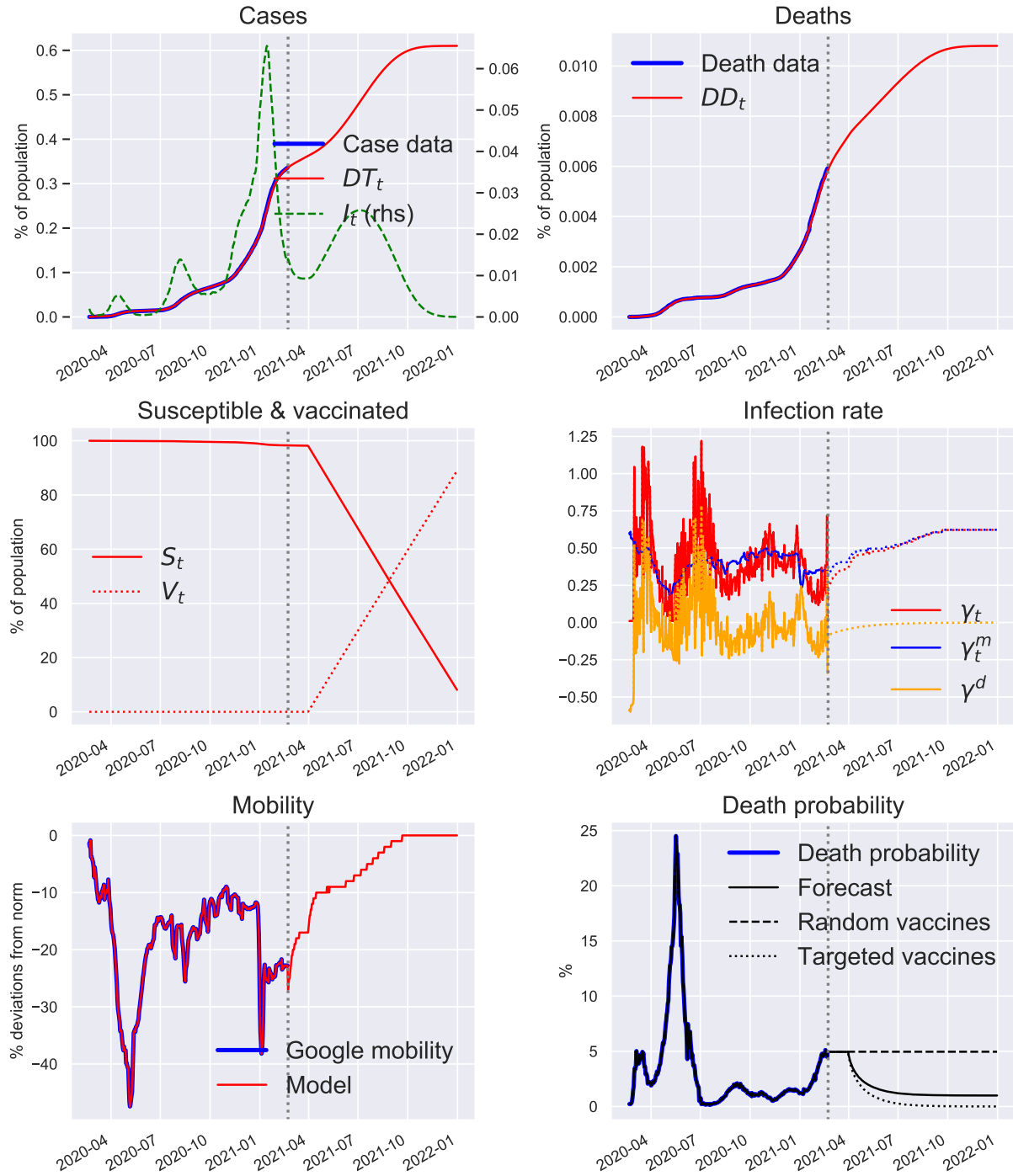
Germany
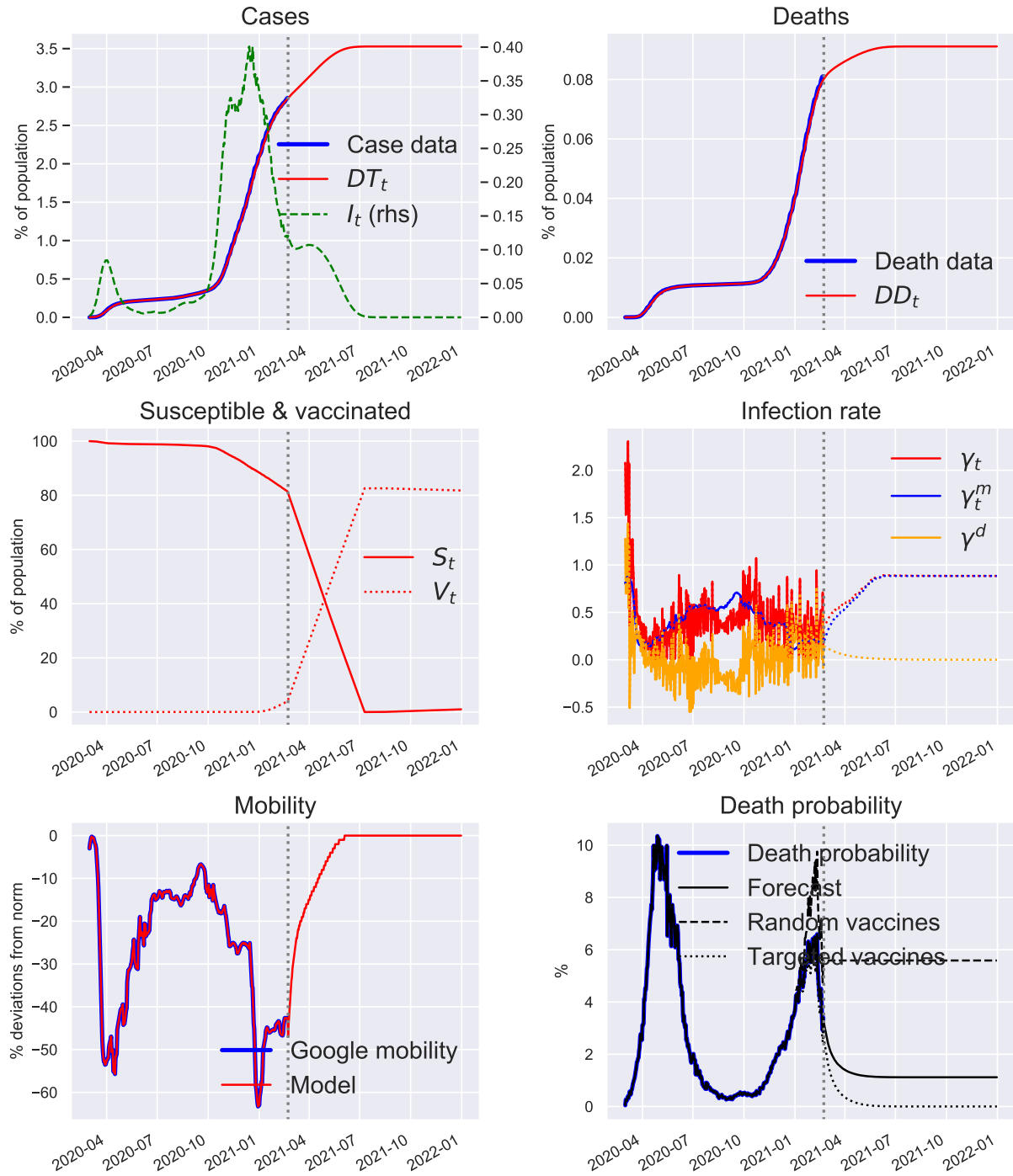
Note: Baseline projections of key epidemiological states and mobility. Assumes steady vaccinations at a pace that will deplete all contracted dosages by end of 2021.

Spain
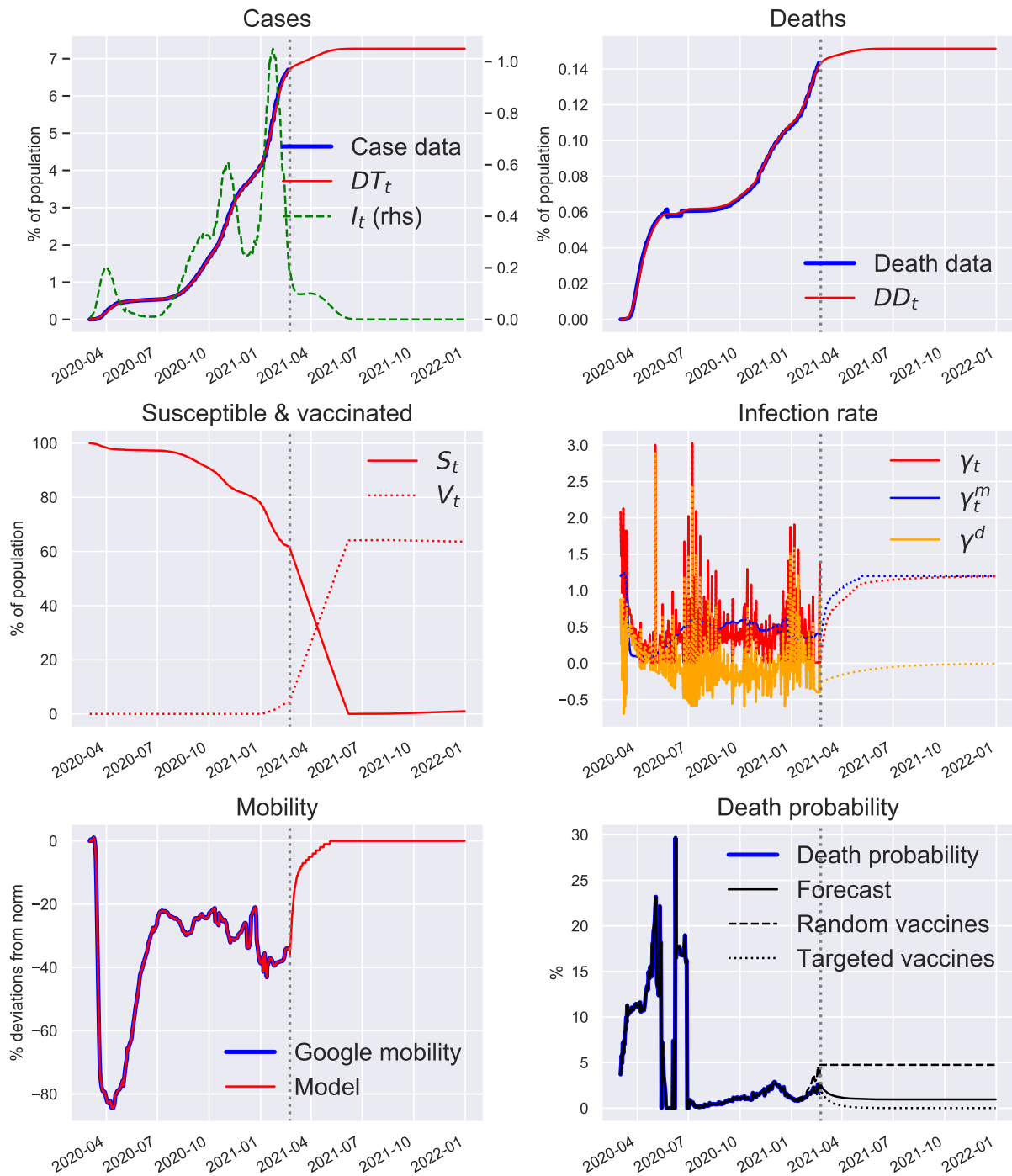
Note: Baseline projections of key epidemiological states and mobility. Assumes steady vaccinations at a pace that will deplete all contracted dosages by end of 2021.
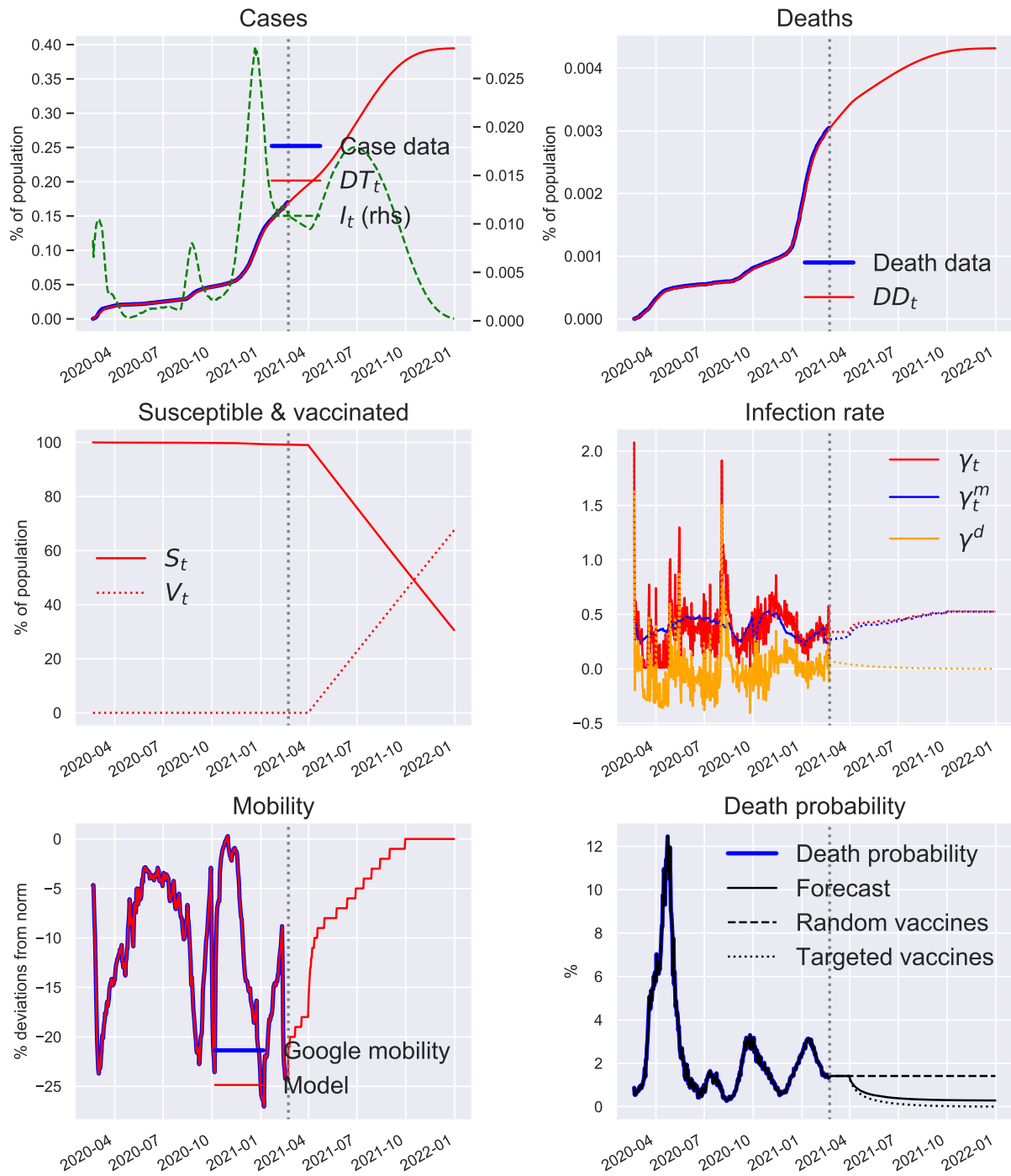
France
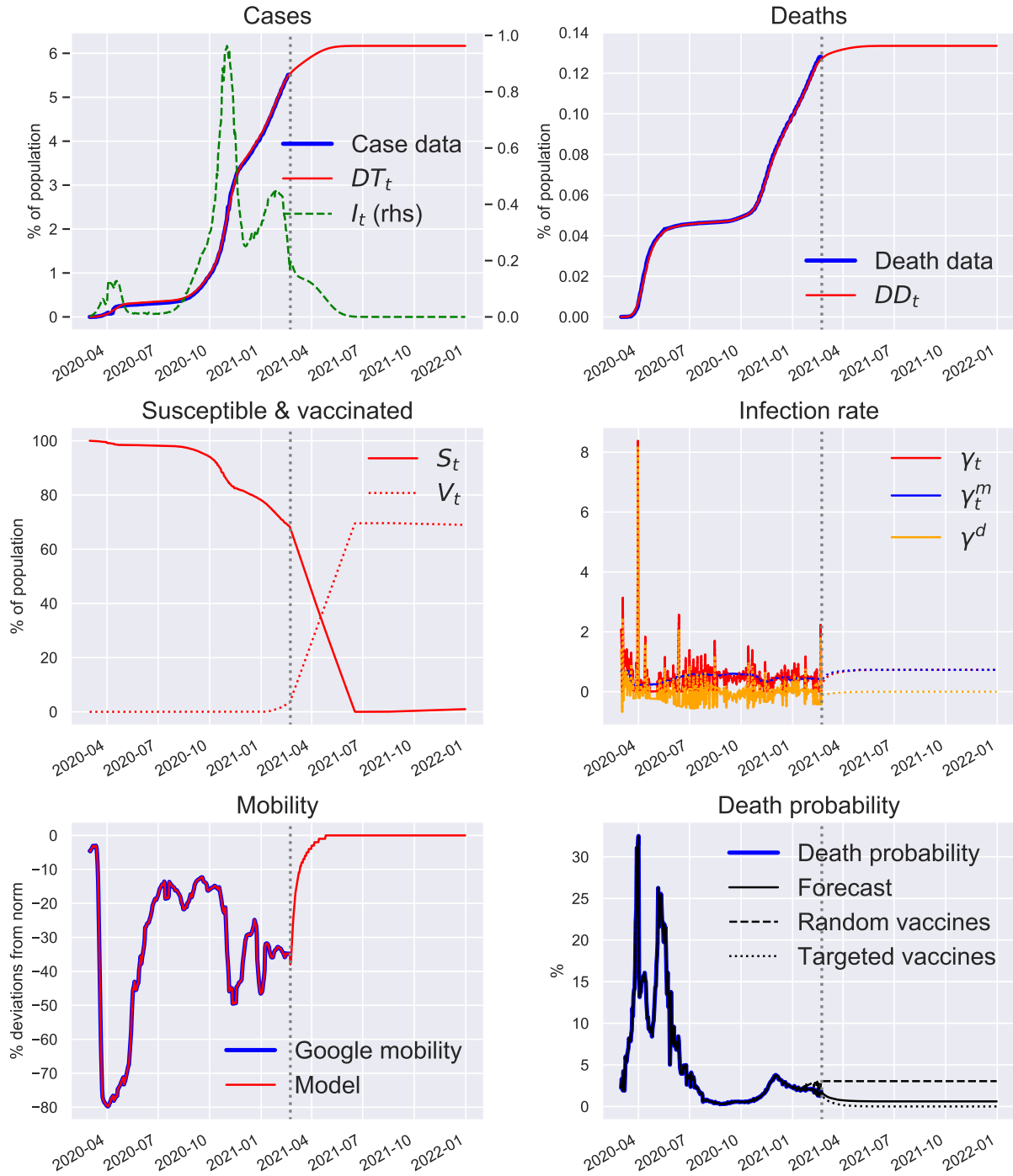
Note: Baseline projections of key epidemiological states and mobility. Assumes steady vaccinations at a pace that will deplete all contracted dosages by end of 2021.

United Kingdom

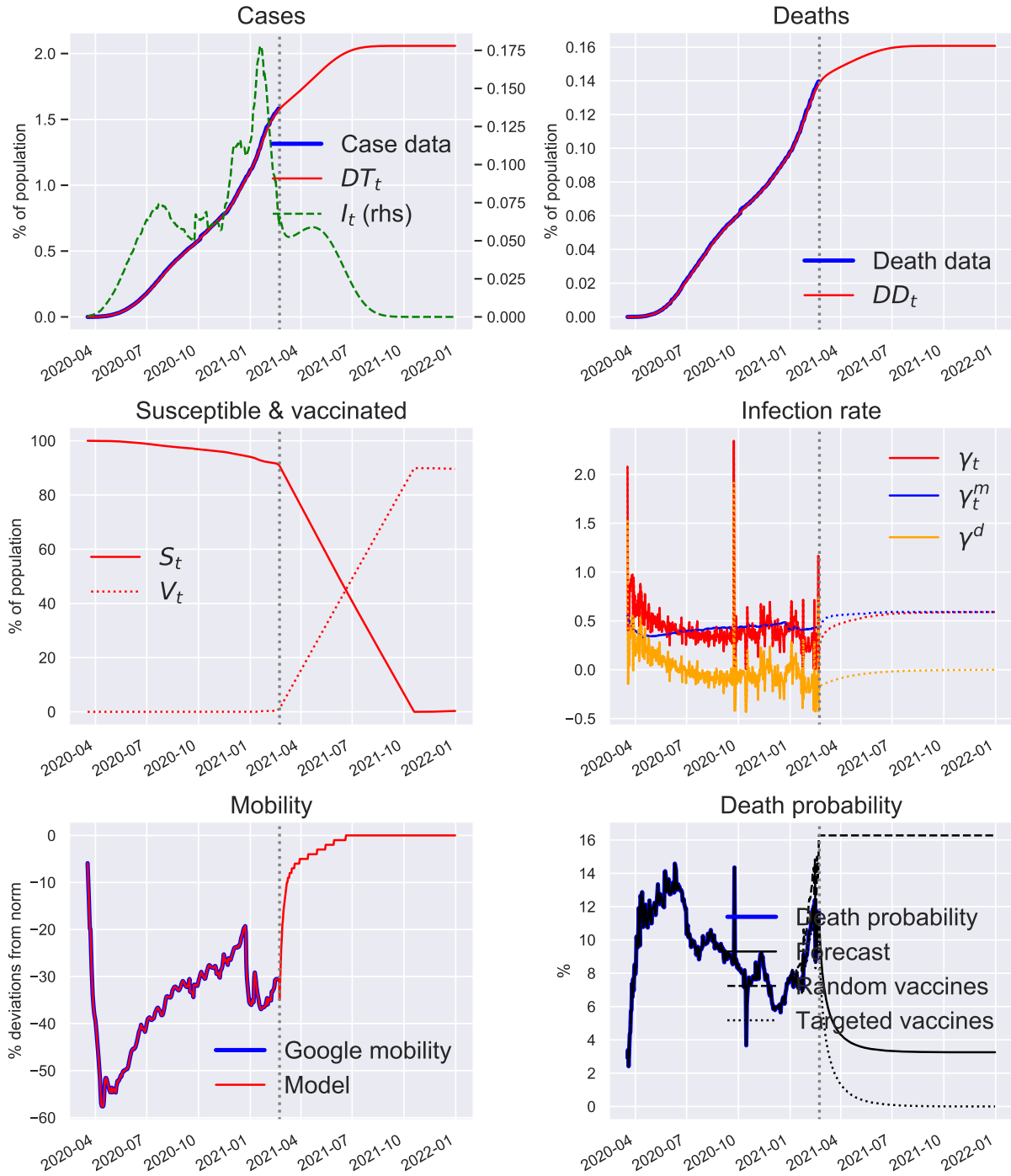**Note**: Baseline projections of key epidemiological states and mobility. Assumes steady vaccinations at a pace that will deplete all contracted dosages by end of 2021.

Indonesia

Cases

Deaths

Susceptible & vaccinated

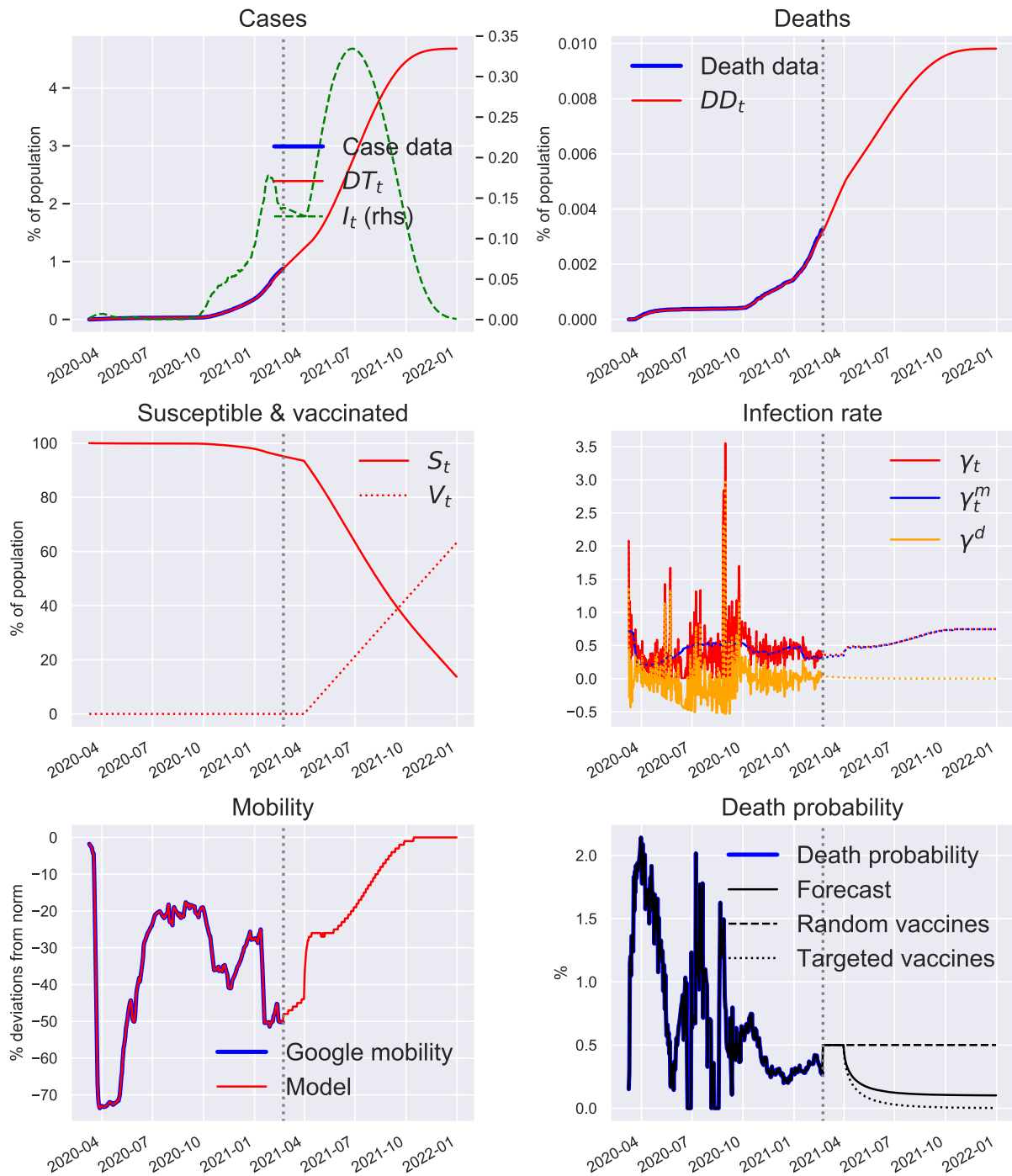### Infection rate

Mobility

Death probability

Note: Baseline projections of key epidemiological states and mobility. Assumes steady vaccinations at a pace that will deplete all contracted dosages by end of 2021.

India

Note: Baseline projections of key epidemiological states and mobility. Assumes steady vaccinations at a pace that will deplete all contracted dosages by end of 2021.

Italy

Cases

Deaths

Susceptible & vaccinated

Infection rate
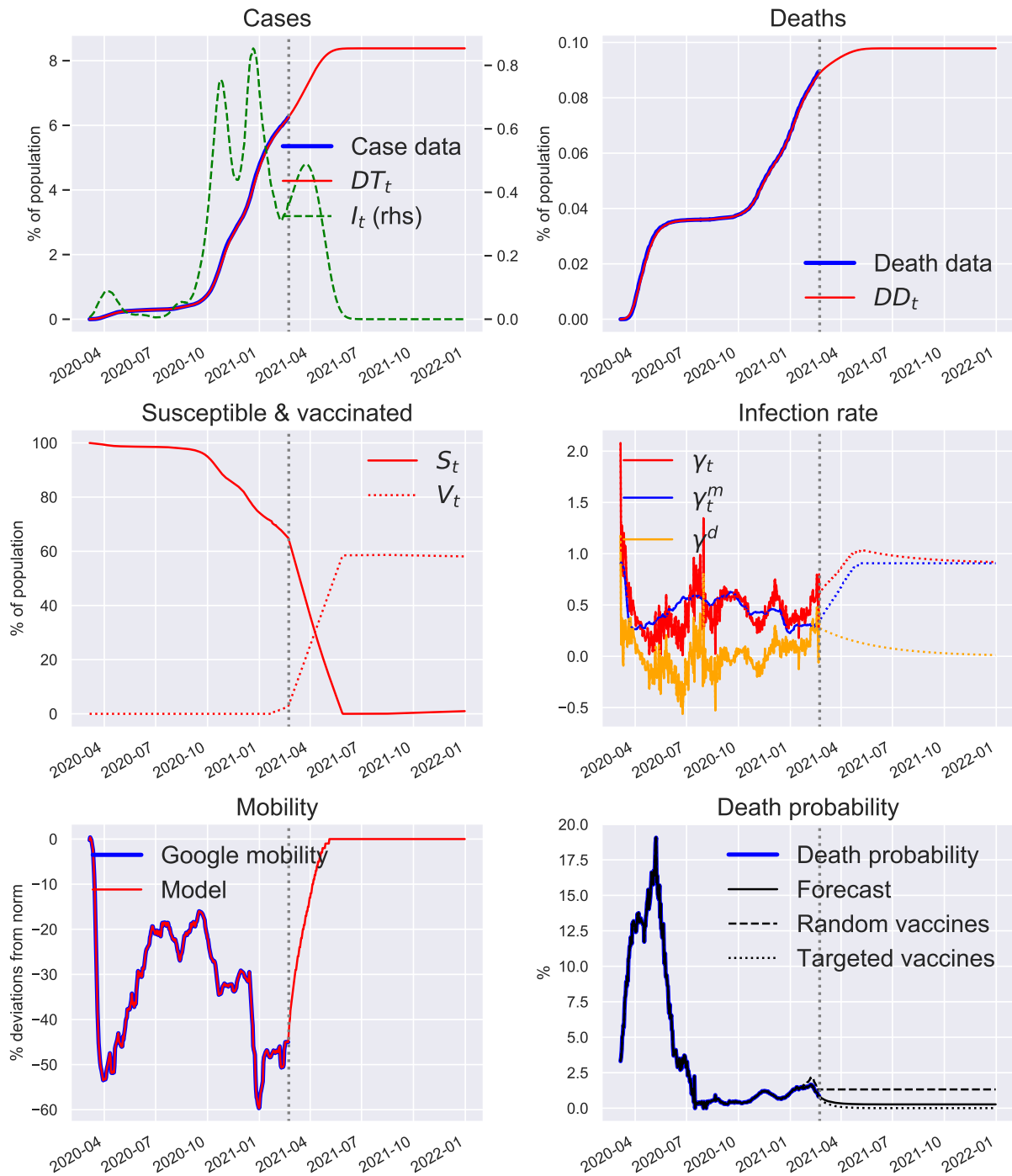
Mobility

Death probability

Note: Baseline projections of key epidemiological states and mobility. Assumes steady vaccinations at a pace that will deplete all contracted dosages by end of 2021.

34

Japan

Cases

Deaths

Susceptible & vaccinated

Infection rate
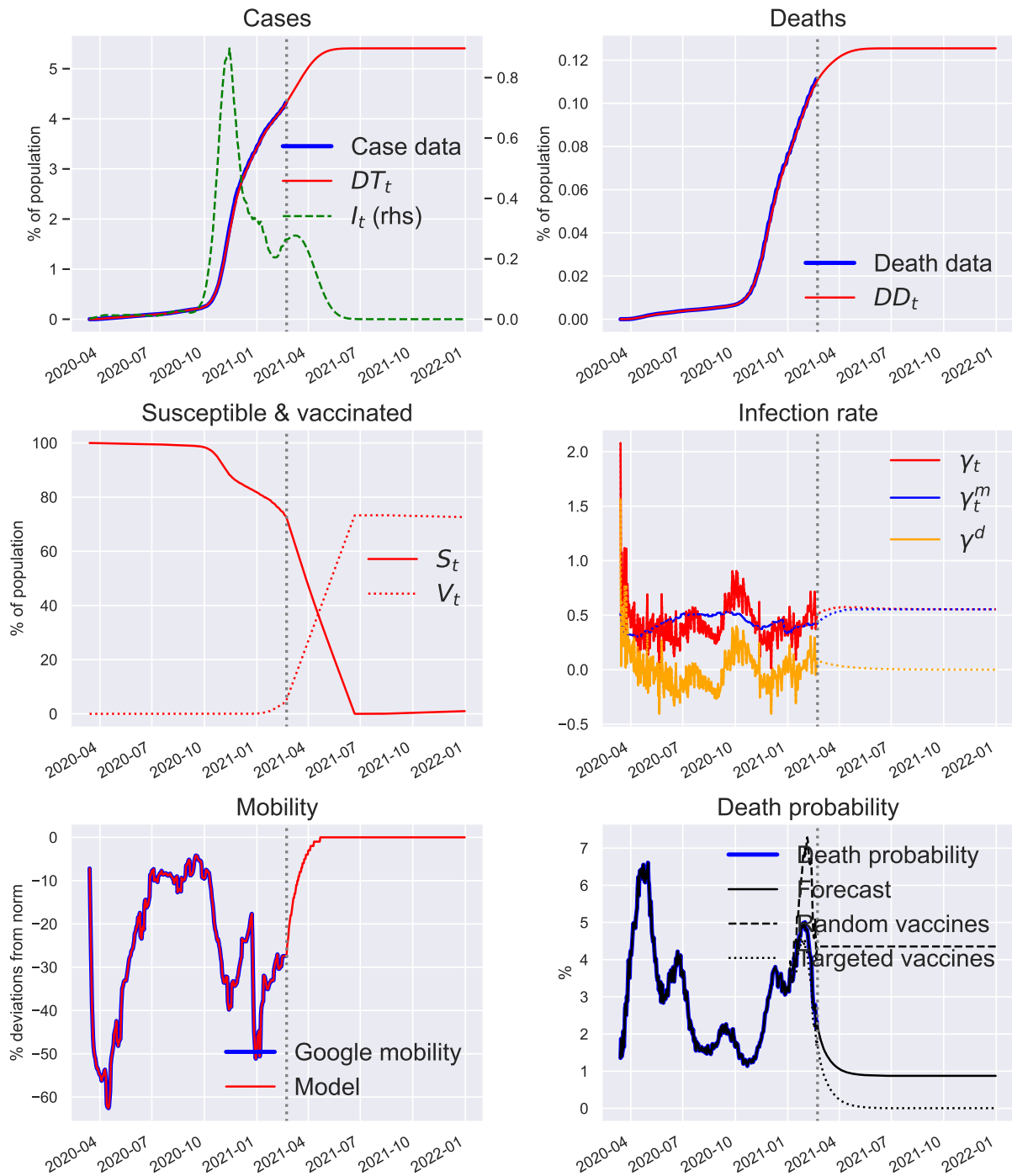

Mobility

Death probability

Note: Baseline projections of key epidemiological states and mobility. Assumes steady vaccinations at a pace that will deplete all contracted dosages by end of 2021.

South Korea

Cases

Deaths

Susceptible & vaccinated

Infection rate
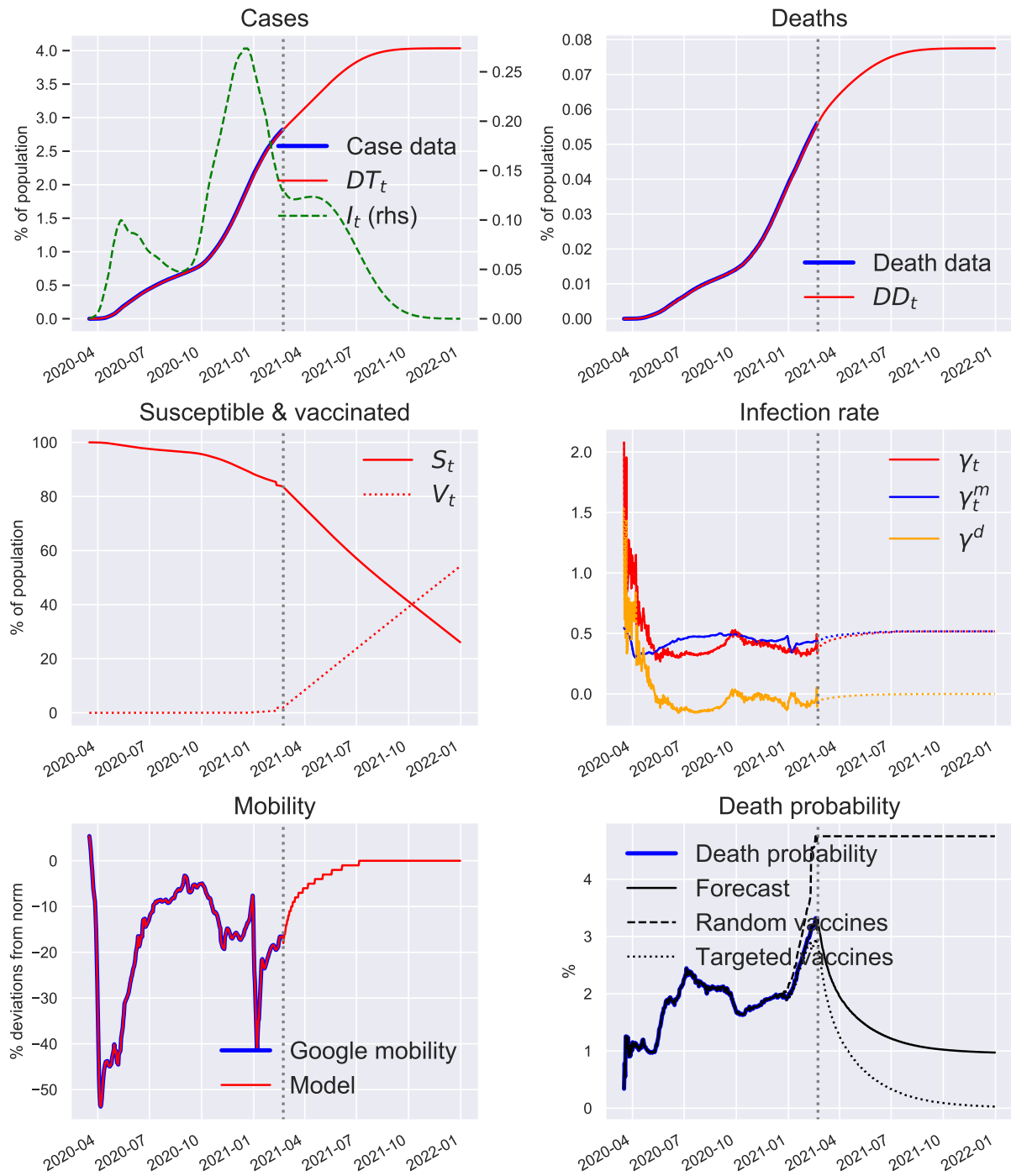

Mobility

Death probability

Note: Baseline projections of key epidemiological states and mobility. Assumes steady vaccinations at a pace that will deplete all contracted dosages by end of 2021.

Mexico

Cases

Deaths

Susceptible & vaccinated

Infection rate
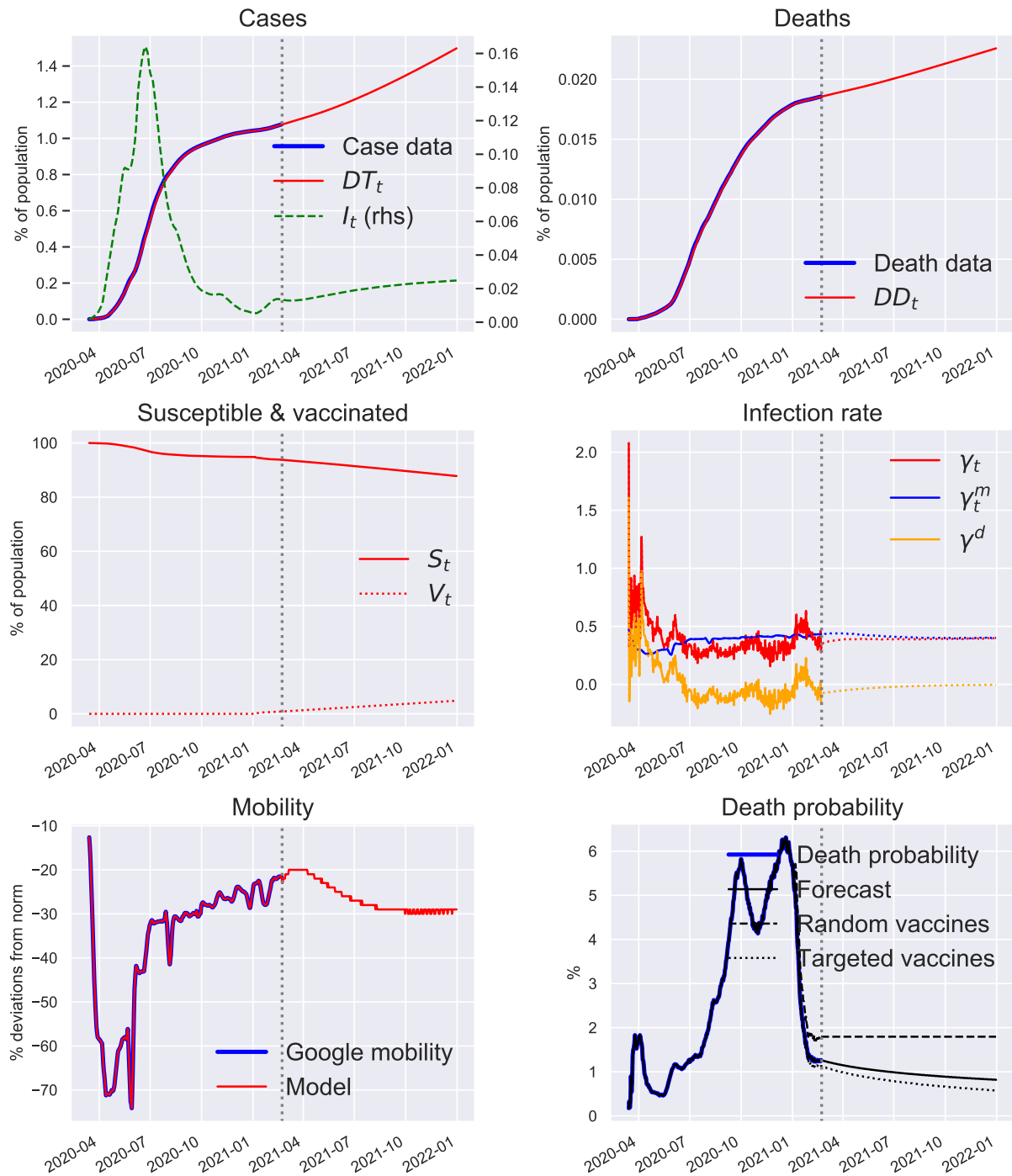

Mobility

Death probability

Note: Baseline projections of key epidemiological states and mobility. Assumes steady vaccinations at a pace that will deplete all contracted dosages by end of 2021.

Malaysia

Cases

Deaths

Susceptible & vaccinated

Infection rate
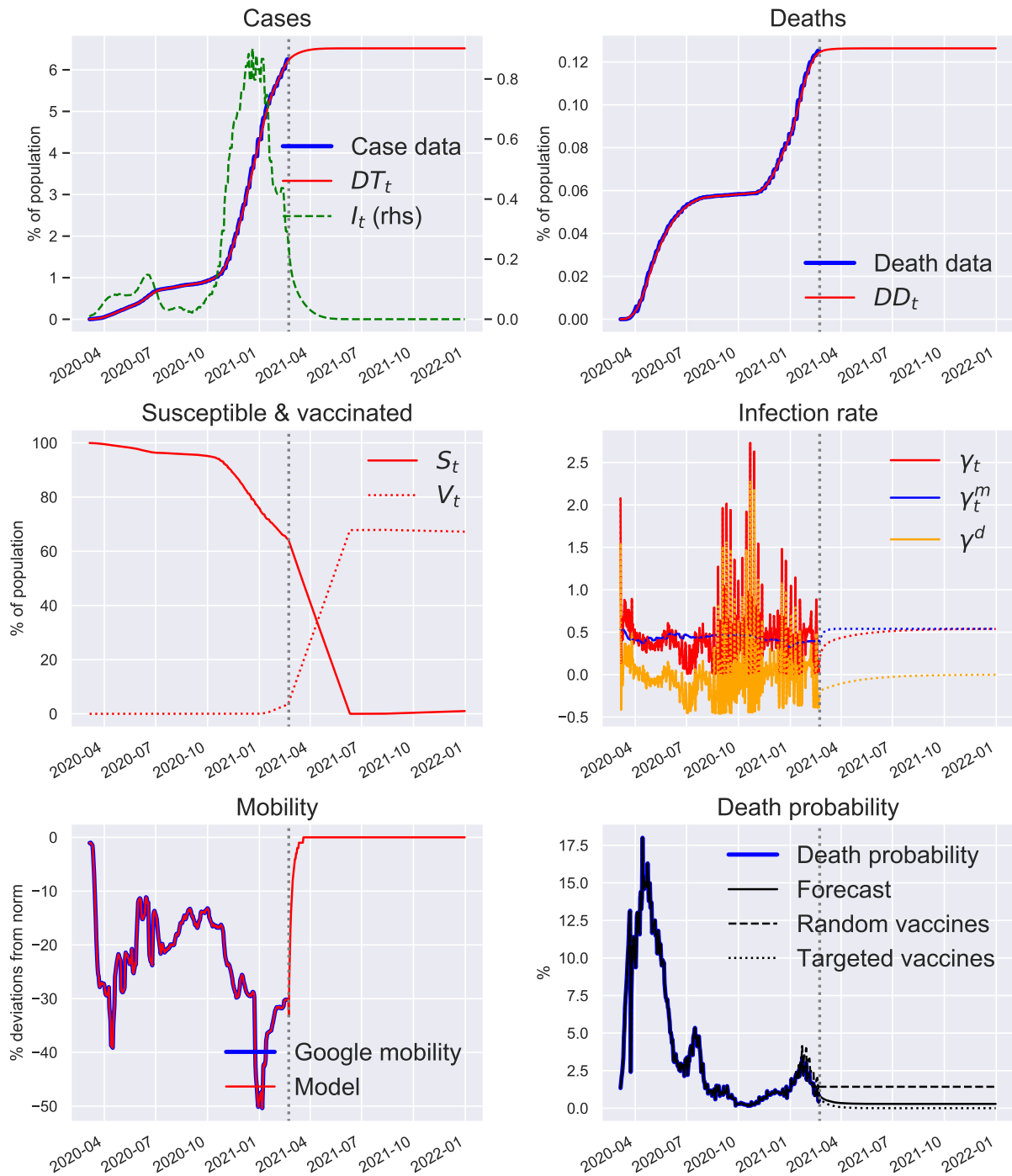
Mobility

Death probability

Note: Baseline projections of key epidemiological states and mobility. Assumes steady vaccinations at a pace that will deplete all contracted dosages by end of 2021.
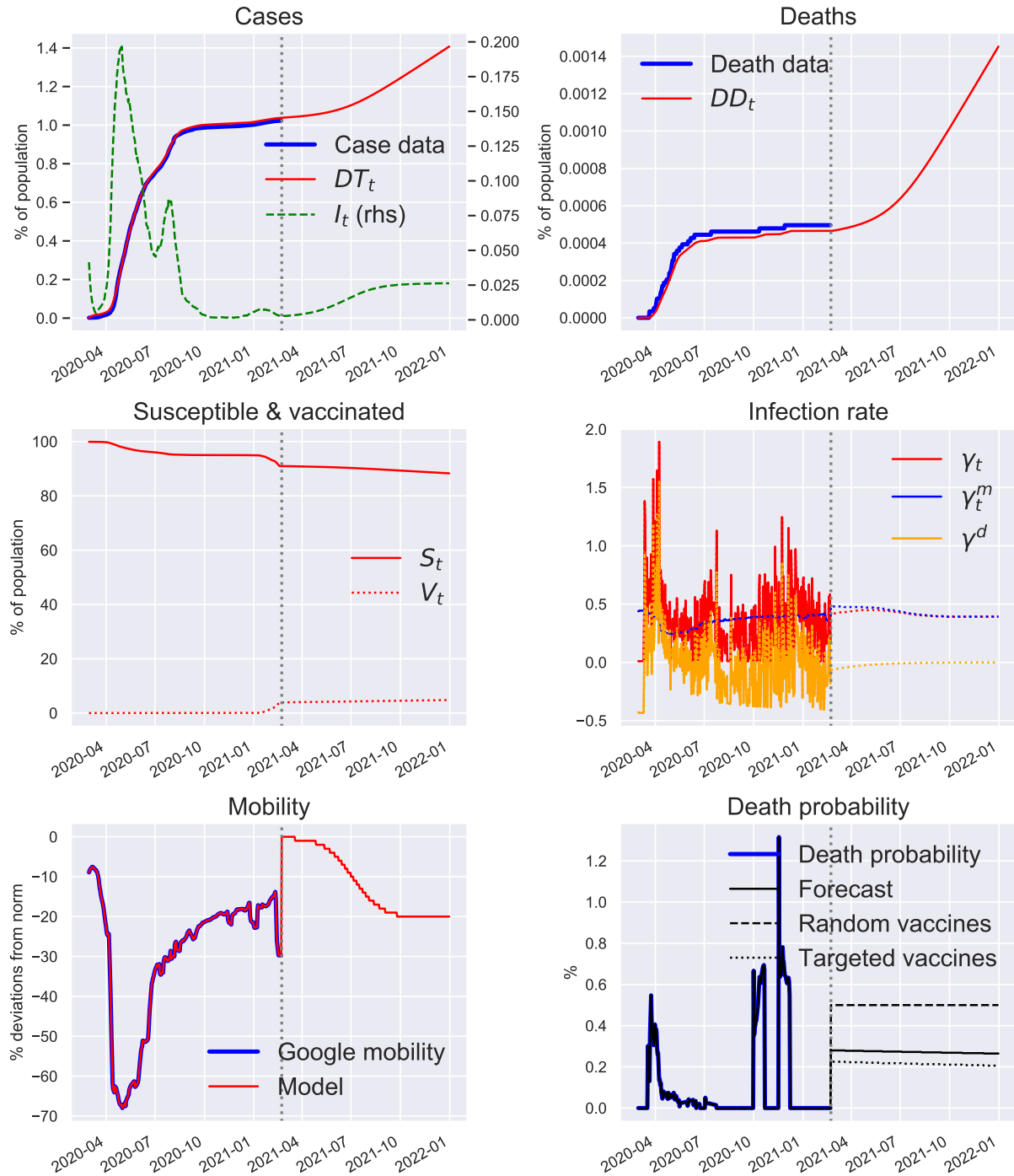
Note: Baseline projections of key epidemiological states and mobility. Assumes steady vaccinations at a pace that will deplete all contracted dosages by end of 2021.

Poland

Note: Baseline projections of key epidemiological states and mobility. Assumes steady vaccinations at a pace that will deplete all contracted dosages by end of 2021.

Russia

Note: Baseline projections of key epidemiological states and mobility. Assumes steady vaccinations at a pace that will deplete all contracted dosages by end of 2021.
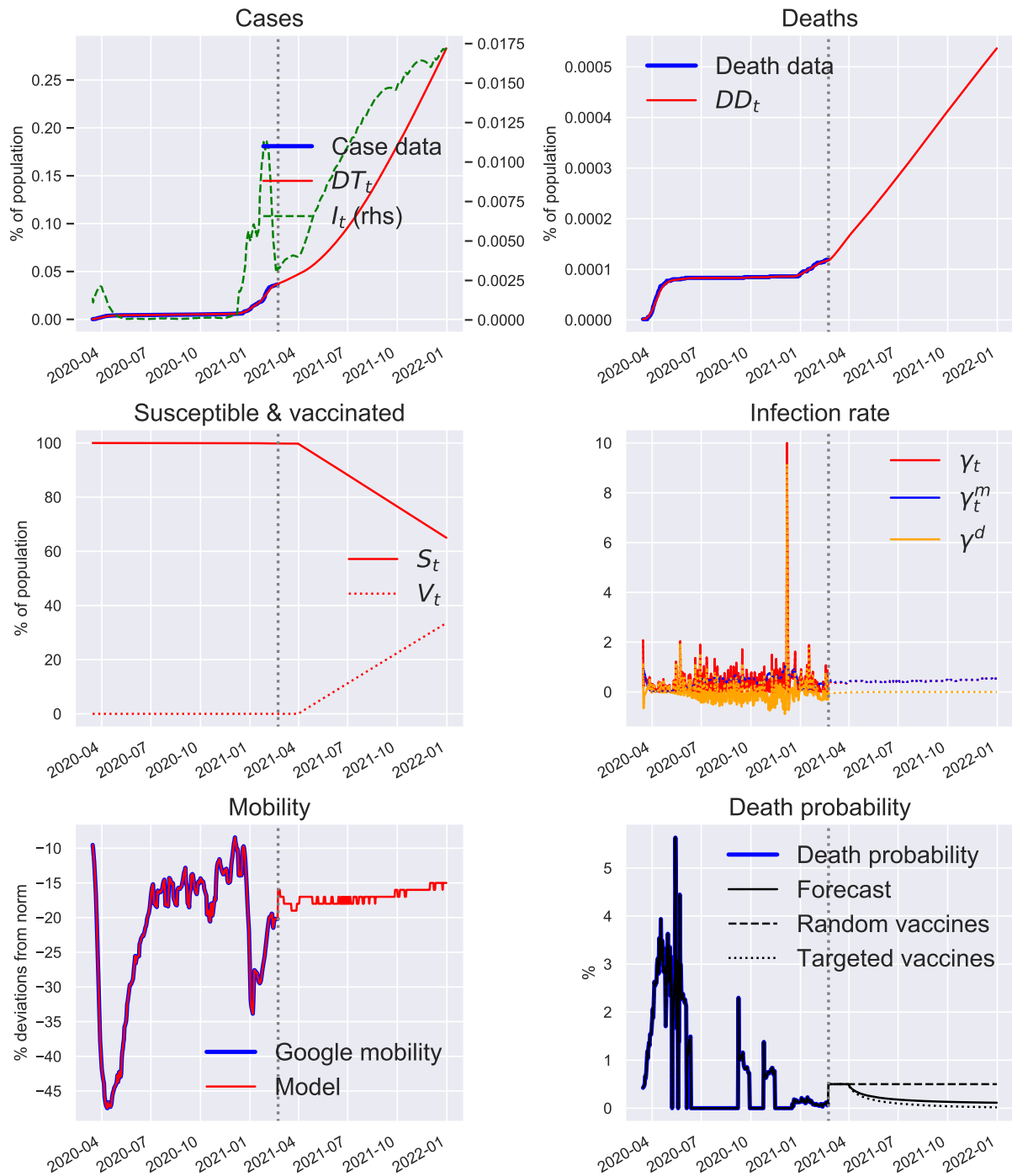
Note: Baseline projections of key epidemiological states and mobility. Assumes steady vaccinations at a pace that will deplete all contracted dosages by end of 2021.
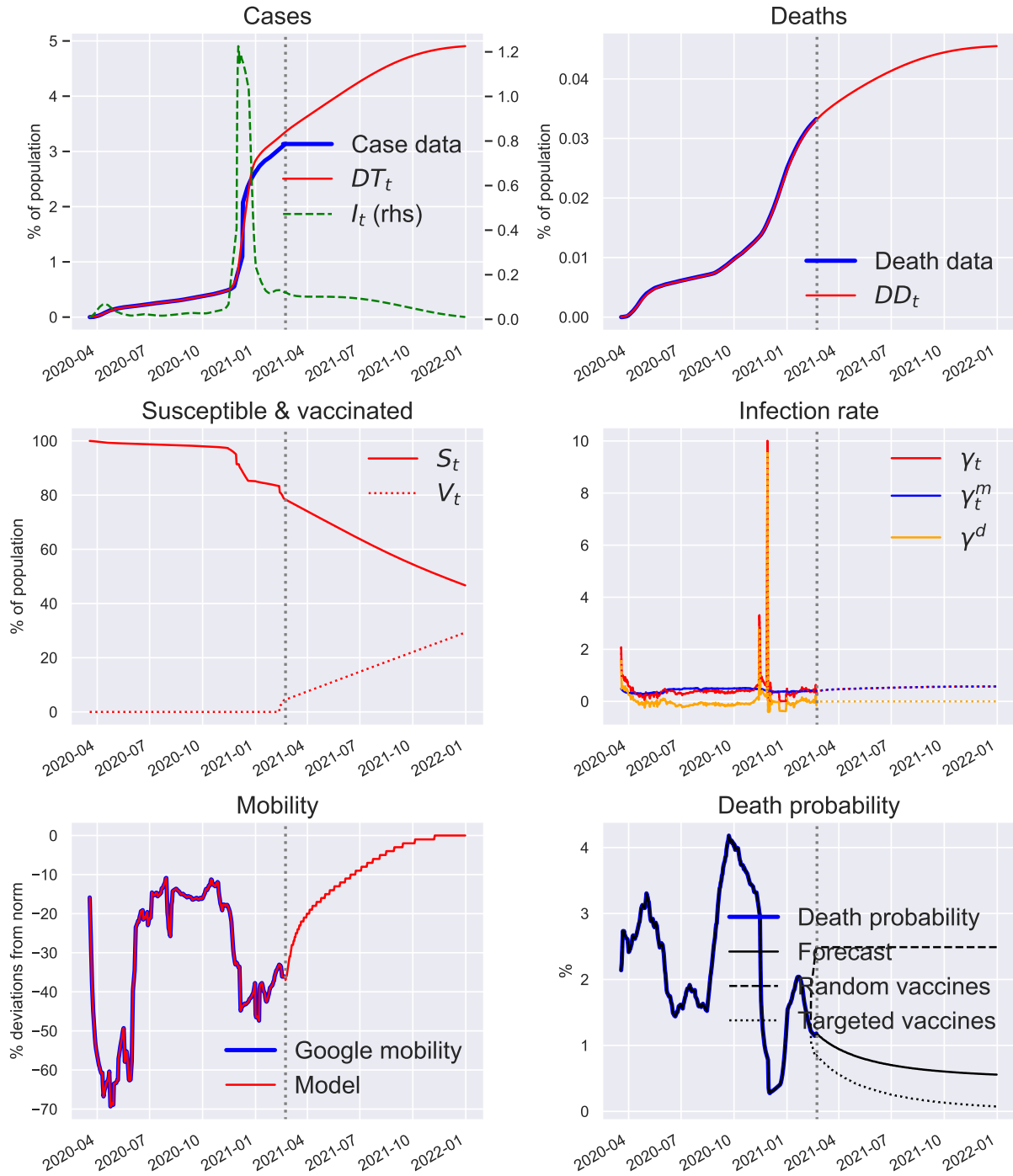
Sweden

Note: Baseline projections of key epidemiological states and mobility. Assumes steady vaccinations at a pace that will deplete all contracted dosages by end of 2021.

Singapore

Cases

Deaths

Susceptible & vaccinated

Infection rate

Mobility

Death probability

Note: Baseline projections of key epidemiological states and mobility. Assumes steady vaccinations at a pace that will deplete all contracted dosages by end of 2021.
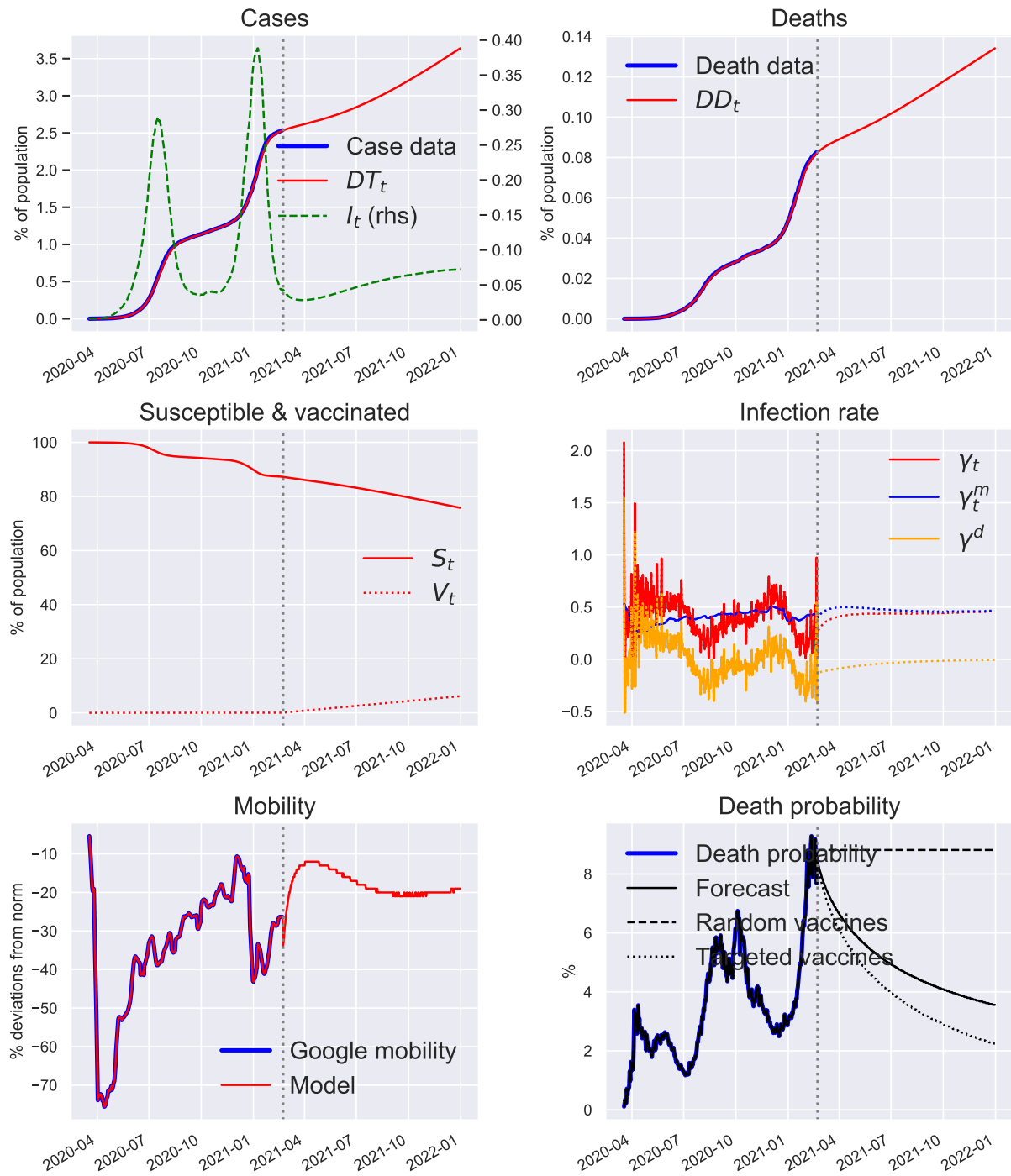
44

Thailand

Note: Baseline projections of key epidemiological states and mobility. Assumes steady vaccinations at a pace that will deplete all contracted dosages by end of 2021.

Turkey

Note: Baseline projections of key epidemiological states and mobility. Assumes steady vaccinations at a pace that will deplete all contracted dosages by end of 2021.

South Africa

Note: Baseline projections of key epidemiological states and mobility. Assumes steady vaccinations at a pace that will deplete all contracted dosages by end of 2021.